

The MSW effect in a fluctuating matter density

A. B. Balantekin* and J. M. Fetter†

Department of Physics, University of Wisconsin at Madison
Madison, WI 53706

F. N. Loreti‡

Institute for Nuclear Theory, University of Washington
Seattle, WA 98195

February 1, 2008

Abstract

We consider the effect on matter-enhanced neutrino flavor transformation of a randomly fluctuating, delta-correlated matter density. The fluctuations will produce a distribution of neutrino survival probabilities. We find the mean and variance of the distribution for the case of solar neutrinos, and discuss the possibility of placing a limit on solar density fluctuations using neutrino data.

1 Introduction

Matter-enhanced neutrino oscillations, especially in connection to the solar neutrino problem [1], have been extensively studied in the recent years. More

*E-mail address: baha@nucsth.physics.wisc.edu

†E-mail address: fetter@nucsth.physics.wisc.edu

‡Present address: Systems for Market Research, Pittsburgh, PA 15229; E-mail address: FNLoreti@aol.com

recently some interest has developed in the problem of neutrino flavor transformations via the Mikheyev-Smirnov-Wolfenstein (MSW) effect in a randomly fluctuating matter density. A general approach to neutrino oscillations in such inhomogeneous matter was developed in Ref. [2]. A Boltzmann-like collision integral with blocking factors, describing the decoherence of neutrinos in matter, was given in Ref. [3]. Matter fluctuations which are not random, but harmonic [4, 5] or changing stepwise [6] were also considered.

Redfield equations for a neutrino traveling in a region with delta-correlated Gaussian noise were recently developed in Ref. [7] and applied to two-neutrino flavor transformations in the post-core bounce supernova environment in Ref. [8]. In parallel to these papers, an analytical procedure to calculate the survival probability was described in Ref. [9], and further implications of solar matter density random noise upon resonant neutrino conversion were studied in Ref. [10].

The aim of this paper is to expand the analysis of Ref. [7] to investigate the mean and variance of the distribution of neutrinos when a randomly-fluctuating, delta-correlated electron density is present in the sun. A general treatment of fluctuations is presented in Section 2. Mean survival probabilities and the variances of the survival probability distribution are given in Sections 3 and 4, respectively. In Section 5, we discuss the results and present conclusions.

2 General Treatment of Fluctuation

We will be concerned with systems whose evolution is described by the Schrödinger-like equation

$$i\frac{\partial}{\partial t}\psi(t) = H(t)\psi(t), \quad (1)$$

where ψ is represented as a column vector. Following the method of Loreti and Balantekin [7], we define the density matrix

$$\rho = \psi \otimes \psi^\dagger \quad (2)$$

and divide H into two parts, one with known time dependence and one which fluctuates with time:

$$H(t) = H_0(t) + B(t)M, \quad (3)$$

where $B(t)$ is a c-number and the operator M does not depend on time.

We assume that the fluctuation $B(t)$ obeys

$$\begin{aligned} \langle B(t_1) \rangle &= 0 \\ \langle B(t_1)B(t_2) \rangle &= \alpha^2 f_{12} \\ \langle B(t_1)B(t_2)B(t_3) \rangle &= 0 \\ \langle B(t_1)B(t_2)B(t_3)B(t_4) \rangle &= \alpha^4 (f_{12}f_{34} + f_{13}f_{24} + f_{14}f_{23}) \\ &\vdots \end{aligned} \quad (4)$$

where $f_{ij} = f(|t_j - t_i|)$ gives the correlation between fluctuations in different places. Throughout the current paper, we will consider the case of delta-

correlated (white) noise:

$$f(x) = 2\tau\delta(x), \quad (5)$$

with the correlation time τ as a parameter. This is equivalent to the statement that the probability of a given $B(t')$ is proportional to

$$\int_0^t \exp\left\{[B(t')]^2/2\tau\alpha^2\right\} dt'. \quad (6)$$

Further, the results from delta correlations will be approximately the same as those from step-function correlations of step length τ as long as we have the constraint

$$\tau \ll \left(C(t) + \frac{d}{dt} \log \alpha(t)\right)^{-1}, \quad (7)$$

where $C(t)$ is the largest element of the matrix commutator $[H_0, M]$. Then we have the following result for the evolution of fluctuation-averaged ρ (cf. Eq. (16) of Ref. [7]):

$$\frac{\partial}{\partial t} \langle \rho(t) \rangle = -\alpha^2 \tau [M, [M, \langle \rho(t) \rangle]] - i[H_0(t), \langle \rho(t) \rangle]. \quad (8)$$

MSW conversion between neutrino flavors obeys the equation

$$i \frac{\partial}{\partial t} \begin{pmatrix} \nu_e \\ \nu_x \end{pmatrix} = \frac{\Delta m^2}{4E} \begin{pmatrix} \zeta(t) - \cos 2\theta & \sin 2\theta \\ \sin 2\theta & -(\zeta(t) - \cos 2\theta) \end{pmatrix} \begin{pmatrix} \nu_e \\ \nu_x \end{pmatrix} \quad (9)$$

where

$$\zeta(t) = \frac{2\sqrt{2}G_F E}{\Delta m^2} N_e(t), \quad (10)$$

θ is the vacuum neutrino mixing angle, Δm^2 is the difference in the squared masses of the two neutrino species, E is the neutrino energy, and N_e is the electron number density.

In order to study the influence of density fluctuations on the conversion rate, one can add periodic matter density perturbations to the average density [4]

$$N_e(r) = \overline{N_e} [1 + \epsilon \sin(kr)], \quad (11)$$

where the wavenumber k is fixed. Such an additional term can induce additional MSW level-crossings giving rise to interference between them. To elucidate this behavior, one can utilize logarithmic perturbation theory, valid for small vacuum mixing angles. The application of logarithmic perturbation theory to the neutrino mixing problem is sketched in the Appendix. If there is more than one MSW resonance point, one can calculate the integral in Eq. (35) to obtain the electron neutrino survival probability, P_e , as

$$P_e = \exp \left[-\frac{\pi \Delta m^2 \sin^2 \theta}{4E} \left| \sum_{t_a} [N'_e(t_a)]^{-1/2} \exp \left[i \int_0^{t_a} \frac{\Delta m^2}{2E} [\zeta(t') - \cos 2\theta] dt' \right] \right|^2 \right] \quad (12)$$

If two turning points are close enough, one can utilize the uniform Airy approximation to obtain

$$P_e = \exp \left[-\pi \frac{\Delta m^2 \sin^2 2\theta}{2E |\zeta'(t_a)|} \sin^2 \left(\frac{\pi}{4} - \frac{\Delta m^2}{4E} \int_{t_a}^{t_b} [\zeta(t) - \cos 2\theta] dt \right) \right], \quad (13)$$

which is the wavenumber dependence observed in Ref. [4].

If the density fluctuations cannot be parameterized with a single wavenumber as given above, but with a distribution of wavenumbers, one can then write

$$N_e(r) = \overline{N_e(r)} [1 + \int dk \epsilon(k) \sin(kr)]. \quad (14)$$

The periodic fluctuation with a given wavenumber k_0 can be recovered by setting $\epsilon(k) = \epsilon\delta(k - k_0)$. The density fluctuations given in Eqs. (5) can then be considered as resulting from stochastically distributed $\epsilon(k)$'s.

3 Calculation of the Mean Survival Probability

We will assume that the electron density N_e fluctuates around the value $\overline{N_e}$, given by the Bahcall-Pinsonneault Standard Solar Model (SSM) including helium diffusion:

$$N_e = (1 + \beta)\overline{N_e} \quad (15)$$

where β fluctuates and obeys constraints similar to those of Eq. (5) with delta correlations.

We may then use the formalism of Section 2 with

$$H_0 = \sigma_z A(t) + \sigma_x B, \quad M = \sigma_z, \quad (16)$$

where we have defined

$$A(t) \equiv \frac{\Delta m^2}{4E}(\overline{\zeta(t)} - \cos 2\theta), \quad B \equiv \frac{\Delta m^2}{4E} \sin 2\theta. \quad (17)$$

Then [7] we have the result

$$\frac{\partial}{\partial t} \begin{pmatrix} r \\ x \\ y \end{pmatrix} = -2 \begin{pmatrix} 0 & 0 & B \\ 0 & k & -A(t) \\ -B & A(t) & k \end{pmatrix} \begin{pmatrix} r \\ x \\ y \end{pmatrix} \quad (18)$$

where

$$k \equiv 2\langle\beta^2\rangle\tau, \quad (19)$$

and

$$\begin{aligned}
r &= 2\langle \nu_e^* \nu_e \rangle - 1 \\
x &= 2 \operatorname{Re} \langle \nu_\mu^* \nu_e \rangle \\
y &= 2 \operatorname{Im} \langle \nu_\mu^* \nu_e \rangle.
\end{aligned} \tag{20}$$

The condition of Eq. (7) now becomes

$$\tau \ll \left(\sin 2\theta \frac{\Delta m^2}{2E} \right)^{-1} \tag{21}$$

where we have assumed that $\log N_e$ varies slowly with time. The right-hand side is the oscillation length of neutrinos at the resonance, divided by 4π . This condition is similar to that of Ref. [10] that $\tau \ll \lambda_m$, the oscillation length of neutrinos at any given point. For definiteness, we will take the correlation length τ to be 10 km. Then the constraint (7) becomes (assuming that the logarithmic derivative is small, which is accurate for the sun)

$$\sin 2\theta \Delta m^2 / E \ll 3.95 \times 10^{-5} \text{ eV}^2 / \text{MeV}. \tag{22}$$

We will present some results for which this condition does not hold, that is, for which the delta correlations we assume would give a different result from step-function correlations. The advantage of a constant correlation length is that the parameter k is constant in $\Delta m^2 / E$, so that we can more meaningfully compare the effects of fluctuations with different MSW parameters than if we let τ vary to satisfy Eq. (7). In any case, since τ and $\langle \beta \rangle_{\text{rms}}$ enter only

through k , one can get identical results to ours by making τ smaller and increasing $\langle\beta\rangle_{\text{rms}}$.

We solved the system (18) numerically; results are presented in Figures 1–3 for $\sin^2 2\theta$ equal to 0.01, 0.1, and 0.7, respectively, and a several values of $\langle\beta\rangle_{\text{rms}}$. 0.01 and 0.7 correspond roughly to the small- and large-mixing solutions [12] to the solar neutrino problem. We used the standard solar model of Bahcall and Pinsonneault, including helium diffusion [11], but assumed all neutrinos were produced at the center of the sun. Usually, fluctuations suppress the $\nu_e \rightarrow \nu_\mu$ transition. For the large-angle solution ($\sin^2 2\theta = 0.7$), the effect on the mean survival probability is noticeable only in the adiabatic region, even in the physically unreasonable case $\langle\beta\rangle_{\text{rms}} = 0.5$. For smaller angles, there is some effect in the non-adiabatic region, but the greatest effect is still in the adiabatic region.

In the adiabatic region, for survival probabilities greater than 1/2, fluctuations tend to enhance the transition. This has been explained [7] by appealing to the flatness of the Bahcall-Pinsonneault density profile near the center. Neutrinos in this region do not go through the resonance point, but do go through part of the resonance region. Travel through that region has a significant effect since the density profile is flat just after production at the center. Fluctuations can therefore have an effect. To confirm that the enhancement depends on the flatness of the density profile, we have also solved the system of equations (18) for an exponential density profile with central

density $6.25 \times 10^{25} \text{ cm}^{-3}$, and scale height $6.21 \times 10^9 \text{ cm}$. These values were chosen to give the same density as the Bahcall-Pinsonneault model at the center and edge of the sun. At $r = R_{\odot}$, we cut the density to zero for both profiles. The exponential results are compared to the Bahcall-Pinsonneault results in Figures 4–6. For fluctuations above about 2%, the exponential profile gives noticeably weaker enhancement of the transition probability than the Bahcall-Pinsonneault profile, and changes the shape of the curve elsewhere as well. This result indicates that large fluctuations can induce appreciable non-adiabatic effects in the adiabatic region, since the initial density is the same in both cases, and both have the same numerical value of final density before the truncation to zero. (In any case, the step should have no effect, since the density at the edge of the sun is much less than the resonant density.)

4 Higher Moments

The formalism developed in Ref. [7] may be used to calculate higher moments of the distribution of survival probabilities. We will present results for the variance of the distribution,

$$\sigma^2 \equiv \langle P_e^2 \rangle - \langle P_e \rangle^2.$$

In principle, the formalism could be used to calculate arbitrary higher moments of the distribution of P_e .

From the evolution equation (9), it is straightforward to show that

$$i \frac{\partial}{\partial t} \begin{pmatrix} \nu_e^* \nu_e \\ \nu_\mu^* \nu_\mu \\ \nu_e \nu_\mu^* \\ \nu_e^* \nu_\mu \end{pmatrix} = \frac{\Delta m^2}{4E} \begin{pmatrix} 0 & (\sigma_x - 1) \sin 2\theta \\ (\sigma_x - 1) \sin 2\theta & 2\sigma_z(\zeta(t) - \cos 2\theta) \end{pmatrix} \begin{pmatrix} \nu_e^* \nu_e \\ \nu_\mu^* \nu_\mu \\ \nu_e \nu_\mu^* \\ \nu_e^* \nu_\mu \end{pmatrix}. \quad (23)$$

As before, we define the density matrix ρ , which now contains the square of the neutrino survival probability, and use the formalism of Section 2 with

$$H_0 = \begin{pmatrix} 0 & (\sigma_x - 1)B \\ (\sigma_x - 1)B & 2\sigma_z A \end{pmatrix}, \quad M = \begin{pmatrix} 0 & 0 \\ 0 & 2\sigma_z \end{pmatrix}. \quad (24)$$

Then in terms of the quantities

$$\begin{aligned} s &= \langle \nu_e^* \nu_e \nu_\mu^* \nu_\mu \rangle = \langle P_e \rangle - \langle P_e^2 \rangle \\ q &= \langle (\nu_e^* \nu_e - \nu_\mu^* \nu_\mu) \nu_\mu^* \nu_e \rangle \\ z &= \langle (\nu_\mu^* \nu_e)^2 \rangle, \end{aligned} \quad (25)$$

we have

$$\frac{\partial}{\partial t} \begin{pmatrix} s \\ q_r \\ q_i \\ z_r \\ z_i \end{pmatrix} = -2 \begin{pmatrix} 0 & 0 & -B & 0 & 0 \\ 0 & k & -A & 0 & B \\ 3B & A & k & -B & 0 \\ 0 & 0 & B & 4k & -2A \\ 0 & -B & 0 & 2A & 4k \end{pmatrix} \begin{pmatrix} s \\ q_r \\ q_i \\ z_r \\ z_i \end{pmatrix} + \begin{pmatrix} 0 \\ 0 \\ B \\ 0 \\ 0 \end{pmatrix}, \quad (26)$$

where the subscripts r and i denote the real and imaginary part of the quantity.

We again solved the system numerically, assuming fluctuations of the same form as in Section 3. The results are presented in Figures 7–9, for the same mixing parameters and values of $\langle \beta \rangle_{\text{rms}}$ as in Figure 1–3. The

quantity plotted is $\sigma \equiv \sqrt{\sigma^2}$, rather than the variance itself. For the smaller angles, there is a dramatic peak in σ around $\Delta m^2/E = 1.6 \times 10^{-5} \text{ eV}^2/\text{MeV}$, corresponding to neutrinos being produced in the resonance region (since we assume that all neutrinos are produced at the center of the sun). The results for $\sin^2 2\theta = 0.7$ show a similar increase around $\Delta m^2/E = 1.6 \times 10^{-6} \text{ eV}^2/\text{MeV}$, which again corresponds to production inside the resonance region. It does not go back down, since the resonance region will include the core for any $\Delta m^2/E$ larger than that.

As the rms noise amplitude increases, the variance seems to saturate at a value of $1/12$, independent of the mixing parameters. Two points are relevant to this phenomenon. First, a uniform probability distribution bounded between zero and one has the same mean and variance. Second, fluctuations will tend to suppress the oscillation of $\langle P_e \rangle$ as a function of time, since it becomes a superposition of oscillations with differing phases. Therefore, we may set the time derivatives on the left-hand sides of Eqs. (18) and (26) to zero. Assuming that k goes to zero smoothly, we are led to the trivial solution $r = 0$ for Eq. (18), and $s = 1/6$ for Eq. (26), where we have taken the limit $k = 0$. This yields a variance of $1/12$ and a mean of $1/2$, as expected.

In order to illustrate the magnitude of the effect, in Figures 10-12, we plot the mean survival probability plus and minus the width σ of the distribution. Note that, even though we did not calculate the higher moments, the mean survival probability plus and minus σ is bounded between zero and one,

suggesting that the distribution of P_e is not very skewed.

5 Discussion

The variance is a potentially important tool for the exploration of solar density fluctuations on some time scales. Fluctuations on the time scale of a radiochemical experiment's run would broaden the distribution of count rates, since different runs would have different survival probabilities. None of the experiments currently operating has noted a broader distribution of rates than expected [13, 14, 15], suggesting that the neutrino data will probably limit, rather than measure, such fluctuations. For the favored, small-angle solution, the variance is strongly peaked when neutrinos are produced near the resonance. This suggests that the finite radial distribution of neutrino production will have an important effect, likely extending the peak to lower values of $\Delta m^2/E$, since those correspond to resonance farther out in the sun. Further, it means that density fluctuations will affect pp neutrinos more strongly than other neutrinos, so that gallium experiments may put the strongest limit on fluctuations.

To develop a very rough estimate of the limit on fluctuations, we note that their effect should become noticeable when the ratio $\sigma/\langle P_e \rangle$ becomes comparable to the relative 1σ experimental uncertainty. To simplify the argument, we assume that the signal observed at the gallium experiment consists only of ~ 0.3 MeV pp neutrinos. (Standard MSW analyses indicate

the near-complete suppression of other neutrinos.) As an example, we will consider the GALLEX results. GALLEX has a 1σ uncertainty of approximately 13% and an energy-averaged survival probability of about 60% [14]. A 1% density fluctuation on the time scale of a GALLEX run, 20 to 28 days, with $\sin^2 2\theta = 0.01$ and $\Delta m^2/E = 1.63 \times 10^{-5} \text{ eV}^2/\text{MeV}$ (chosen to give a 60% survival probability), has $\sigma/\langle P_e \rangle = 0.15$. It is likely, then, that a careful study could rule out fluctuations on that level.

In the future, real-time, high-statistics detectors such as HELLAZ [16] and Borexino [17] could be used to investigate fluctuations on shorter time scales. In particular, a helioseismological g-mode oscillation could leave a signature in the neutrino data. Unfortunately, the current high-statistics experiments SNO [18] and Super-Kamiokande [19] probably cannot be used to probe fluctuations in this way, as they are not sensitive to low-energy neutrinos.

A proper averaging over neutrino production location would be extremely cpu-intensive. In this regard, approximate analytic techniques to compute the moments of the density matrix, such as that of Ref. [9], may be very useful in analyzing data.

Acknowledgments

We thank John Beacom, George Fuller, and Y.-Z. Qian for useful conversations. This research was supported in part by the U.S. National Science

Foundation Grant No. PHY-9314131 at the University of Wisconsin, in part the Department of Energy under Grant No. DE-FG06-90ER40561 at the Institute for Nuclear Theory, and in part by the University of Wisconsin Research Committee with funds granted by the Wisconsin Alumni Research Foundation.

Appendix

Here we summarize the application of logarithmic perturbation theory to a two level system [20]. Consider

$$i \frac{\partial}{\partial t} \begin{pmatrix} \psi_1 \\ \psi_2 \end{pmatrix} = \begin{pmatrix} A & gC \\ gC & A \end{pmatrix} \begin{pmatrix} \psi_1 \\ \psi_2 \end{pmatrix} \quad (27)$$

subject to the initial condition $\psi_1(t=0) = 1$ and $\psi_2(t=0) = 0$. Defining

$$z \equiv \frac{\psi_2}{\psi_1} \quad (28)$$

we find that the quantity z satisfies the Riccati equation,

$$i \dot{z} = -2Az + gC(1 - z^2). \quad (29)$$

Expanding z in powers of g

$$z = z_0 + gz_1 + g^2 z_2 + \dots, \quad (30)$$

inserting into Eq. (29), and equating powers of g , we find that

$$z = -ig e^{+2i \int_0^t A(t') dt'} \int_0^t dt' C(t') e^{-2i \int_0^{t'} A(t'') dt''} + \mathcal{O}(g^3) \quad (31)$$

is the solution with the given initial conditions. In order to calculate the survival probability, $|\psi_1|^2$, we observe that

$$|\psi_1|^2 = \frac{1}{1 + |z|^2}, \quad (32)$$

where we have used $|\psi_1|^2 + |\psi_2|^2 = 1$. It is easy to show that Eq. (29) can be rewritten as

$$i \frac{d}{dt} \log(1 + |z|^2) = gC(z^* - z). \quad (33)$$

Eqs. (32) and (33) then yield

$$|\psi_1|^2 = \exp \left[2g \int_0^T dt C(t) \operatorname{Im} z \right]. \quad (34)$$

Finally, substituting the approximate solution, Eq. (31), into Eq. (34), we arrive at the desired answer:

$$|\psi_1|^2 = \exp \left[-\frac{g^2}{2} \left| \int_0^T dt C(t) e^{+2i \int_0^t A(t') dt'} \right|^2 + \mathcal{O}(g^4) \right]. \quad (35)$$

It usually is possible to calculate the integral in Eq. (35) within the stationary phase approximation. If the quantities $A(t)$ and $C(t)$ are monotonically changing, there is only one stationary point t_a and we can approximate the integral above as

$$|\psi_1|^2 = \exp \left[-\pi g^2 \frac{C^2(t_a)}{A'(t_a)} + \mathcal{O}(g^4) \right], \quad (36)$$

where the prime denotes the derivative with respect to time. In most cases, especially when $A(t)$ fluctuates, there could be more than one turning point.

If two of the turning points are close to each other it would be necessary to employ the Airy uniform approximation [21]. In this case one gets

$$|\psi_1|^2 = \exp \left[\frac{-\pi^2 g^2}{2} \left| \left(\frac{C(t_a)}{\sqrt{|A'(t_a)|}} + \frac{C(t_b)}{\sqrt{|A'(t_b)|}} \right) \zeta^{1/4} \text{Ai}(-\zeta) - i \left(\frac{C(t_a)}{\sqrt{|A'(t_a)|}} - \frac{C(t_b)}{\sqrt{|A'(t_b)|}} \right) \zeta^{-1/4} \text{Ai}'(-\zeta) \right|^2 + \mathcal{O}(g^4) \right], \quad (37)$$

where t_a and t_b are the turning points, $\text{Ai}(x)$ and $\text{Ai}'(x)$ are the Airy function and its derivative, and

$$\zeta = \left[-\frac{3}{2} \int_{t_a}^{t_b} A(t) dt \right]^{2/3}. \quad (38)$$

If the turning points are far apart, one can simplify Eq. (37) using the asymptotic expressions of the Airy function:

$$|\psi_1|^2 = \exp \left[-2\pi g^2 \frac{C^2(t_a)}{|A'(t_a)|} \sin^2 \left(\frac{\pi}{4} - \int_{t_a}^{t_b} A(t) dt \right) \right], \quad (39)$$

where we have assumed that the functions $C(t)$ and $A'(t)$ are very slowly changing in this interval, i.e. $C(t_a) = C(t_b)$ and $A'(t_a) = A'(t_b)$.

References

- [1] For a recent review see *Solar Modeling*, A.B. Balantekin and J.N. Bahcall, Eds. (World Scientific, Singapore, 1995).
- [2] R. F. Sawyer, Phys. Rev. D **42**, 3908 (1990).
- [3] G. Raffelt, G. Sigl, and L. Stodolsky, Phys. Rev. Lett. **70**, 2363 (1993).
- [4] A. Schafer and S. E. Koonin, Phys. Lett. B **185**, 417 (1987).
- [5] W.C. Haxton and W.-M. Zhang, Phys. Rev. D **43**, 2484 (1991).
- [6] P. I. Krastev and A. Yu. Smirnov, Mod. Phys. Lett. **6**, 1001 (1991);
Phys. Lett. B **226**, 341 (1989).
- [7] F. N. Loreti and A. B. Balantekin, Phys. Rev. D **50**, 4762 (1994).
- [8] F. N. Loreti, Y.-Z. Qian, G. M. Fuller, and A. B. Balantekin, Phys. Rev. D **52**, 6664 (1995).
- [9] E. Torrente Lujan, hep-ph/9602398.
- [10] H. Nunokawa, A. Rossi, V. B. Semikoz and J. W. F. Valle, hep-ph/9602307.
- [11] J. N. Bahcall and M. H. Pinsonneault, Rev. Mod. Phys. **64**, 885 (1992);
ibid. **67**, 781 (1995).

- [12] S. A. Bludman, N. Hata, D. C. Kennedy, and P. G. Langacker, Phys. Rev. D **47**, 2220 (1993).
- [13] J. N. Abdurashitov et al., Phys. Lett. B **328**, 234 (1994); *ibid.* Nucl. Phys. B (Proc. Suppl.) **38**, 60 (1995).
- [14] P. Anselmann et al., Phys. Lett. B **314**, 445 (1993); *ibid.* **B357**, 237 (1995).
- [15] R. Davis, Prog. Part. Nucl. Phys. **32**, 13 (1994).
- [16] G. Bonvicini, Nucl. Phys. B (Proc. Suppl.) **35**, 438 (1994); T. Ypsilantis et al., LPC-92-31.
- [17] M. C. Giammarchi, Nucl. Phys. B (Proc. Suppl.) **35**, 433 (1994); C. Arpesella et al., Borexino proposal (1991).
- [18] G. Ewan et al., Nucl. Inst. Meth. A **314**, 373 (1992); Phys. in Canada **48**, 112 (1992).
- [19] Y. Suzuki, Nucl. Phys. B (Proc. Suppl.) **35**, 273 (1994);
- [20] A.B. Balantekin, S.H. Fricke, and P.J. Hatchell, Phys. Rev. D **38**, 935 (1989).
- [21] C. Chester, B. Friedman, and F. Ursell, Proc. Cambridge Philos. Soc. **53**, 599 (1957); S. H. Fricke, A. B. Balantekin, and T. Uzer, J. Math. Phys. **32**, 3125 (1991).

Figure Captions

Figure 1. Mean survival probability for a Bahcall-Pinsonneault density profile and $\sin^2 2\theta = 0.01$. The probability is plotted for $\langle\beta\rangle_{\text{rms}}$ equal to 0, 0.01, 0.02, 0.04, 0.08, and 0.5, with a constant correlation length $\tau = 10$ km.

Figure 2. As Figure 1, but with $\sin^2 2\theta = 0.1$. The vertical dotted line indicates where the constraint of Equation (22) begins to break down; there, $\sin 2\theta \Delta m^2/E = 0.1 \times (3.95 \times 10^{-5}) \text{ eV}^2/\text{MeV}$.

Figure 3. As Figure 1, but with $\sin^2 2\theta = 0.7$. The vertical dotted line is as in Figure 2.

Figure 4. Mean survival probability for the Bahcall-Pinsonneault sun compared to an exponential density profile with the same central and edge density, with $\sin^2 2\theta = 0.01$. (a)-(e) show $\langle\beta\rangle_{\text{rms}}$ equal to 0, 0.01, 0.02, 0.04, and 0.08, respectively. The solid line is the Bahcall-Pinsonneault sun, and the dashed line is the exponential.

Figure 5. As Figure 4, but with $\sin^2 2\theta = 0.1$. The vertical dotted line is as in Figure 2.

Figure 6. As Figure 4, but with $\sin^2 2\theta = 0.7$. The vertical dotted line is as in Figure 2.

Figure 7. σ for a Bahcall-Pinsonneault density profile, with the same values of $\sin^2 2\theta$ and $\langle\beta\rangle_{\text{rms}}$ as Figure 1.

Figure 8. As Figure 7, but with $\sin^2 2\theta = 0.1$. The vertical dotted line is as in Figure 2.

Figure 9. As Figure 7, but with $\sin^2 2\theta = 0.7$. The vertical dotted line is as in Figure 2.

Figure 10. Mean survival probability plus and minus σ for the Bahcall-Pinsonneault density profile with $\sin^2 2\theta = 0.01$. (a)-(d) show $\langle\beta\rangle_{\text{rms}}$ equal to 0.01, 0.02, 0.04, and 0.08, respectively.

Figure 11. As Figure 10, but with $\sin^2 2\theta = 0.1$.

Figure 12. As Figure 10, but with $\sin^2 2\theta = 0.7$.

Figure 1

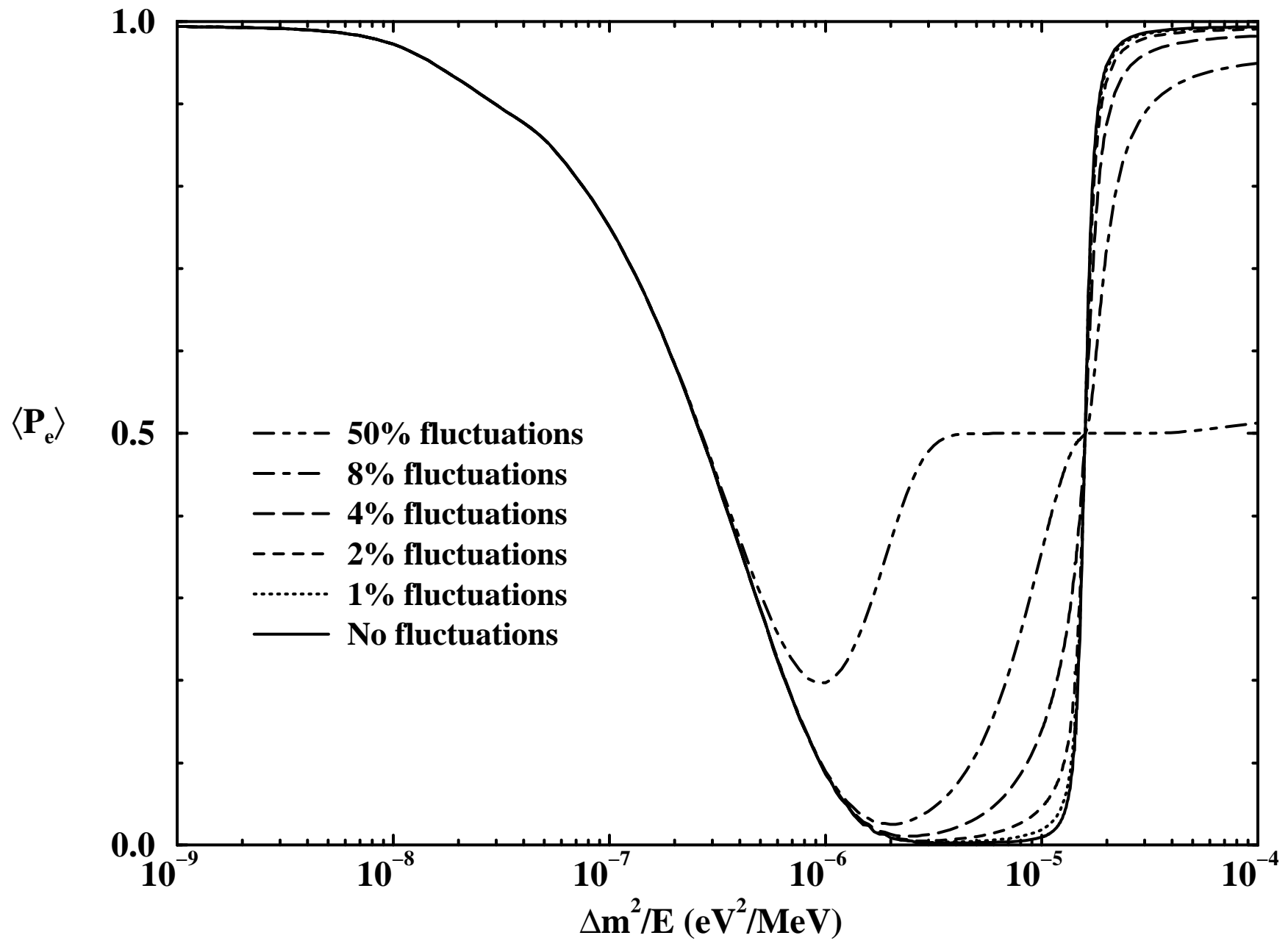


Figure 2

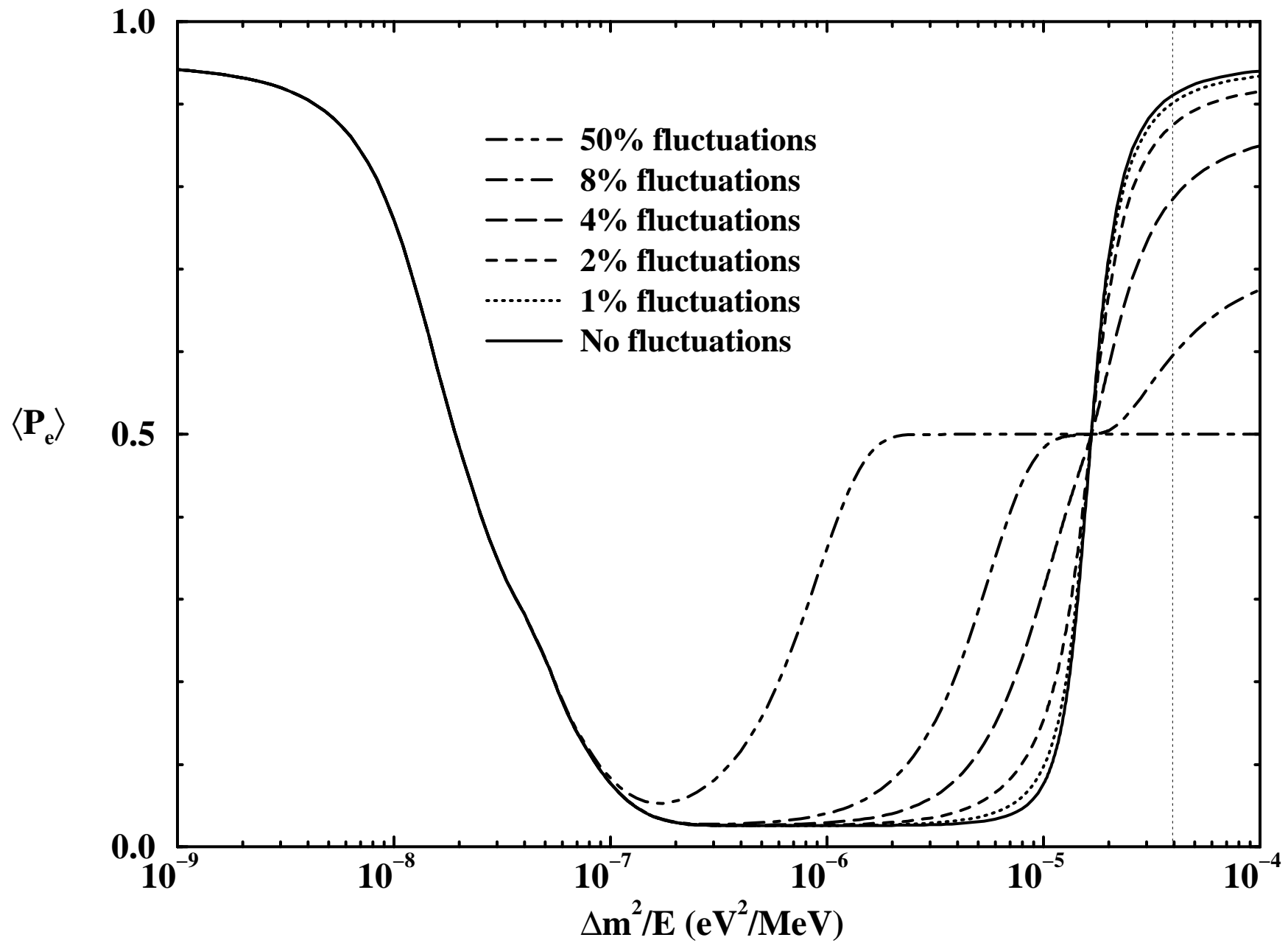


Figure 3

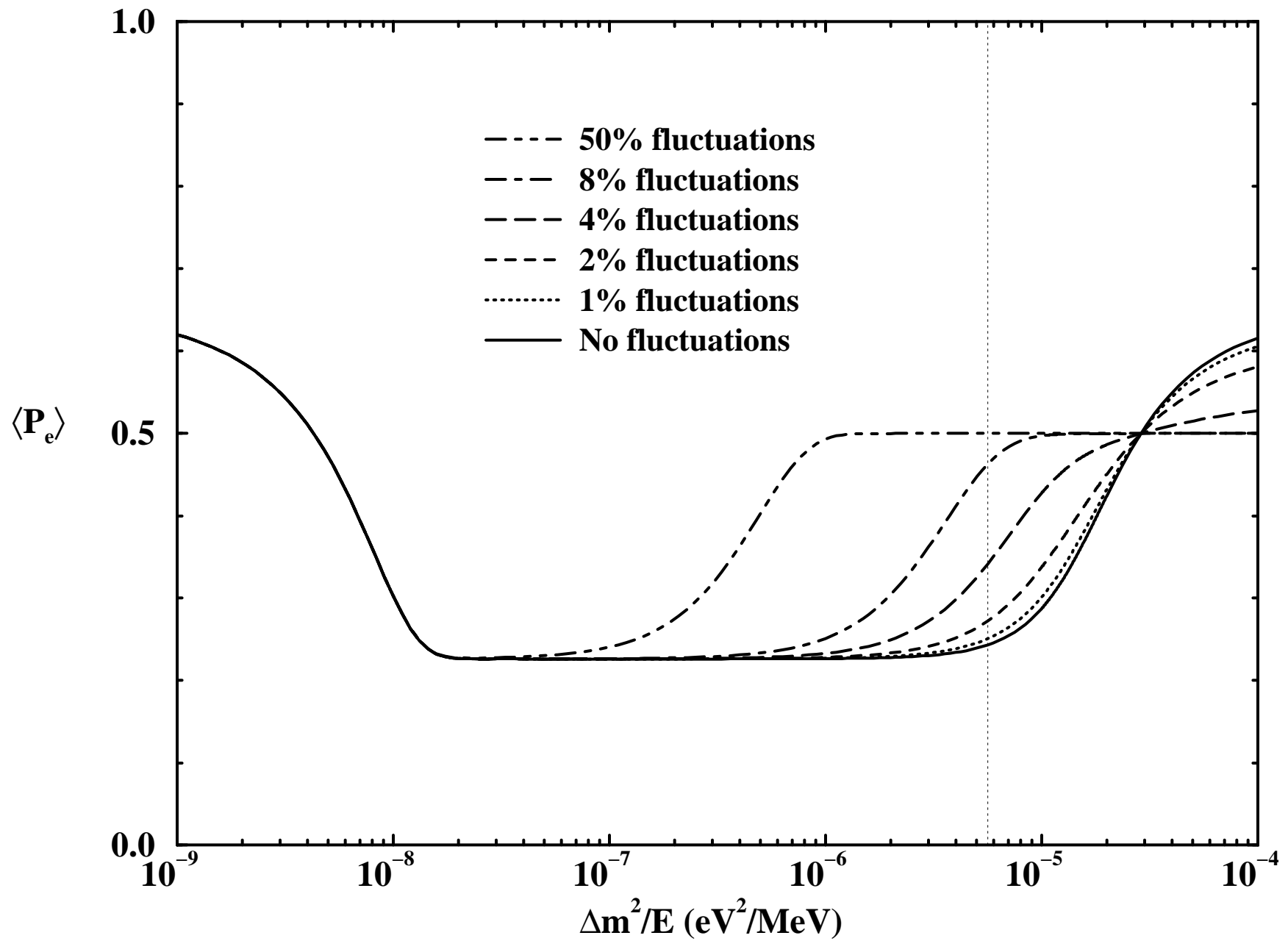


Figure 4a

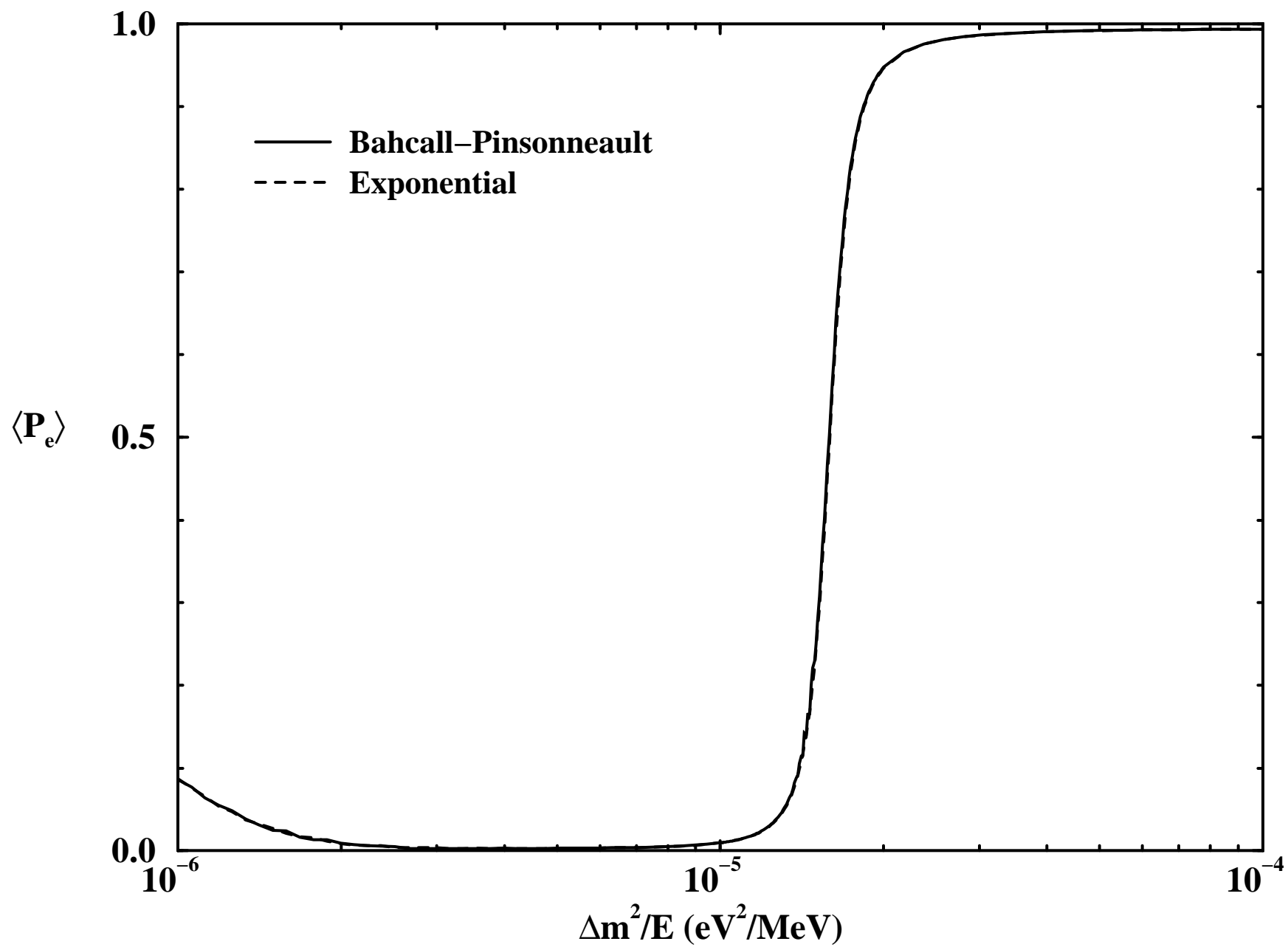


Figure 4b

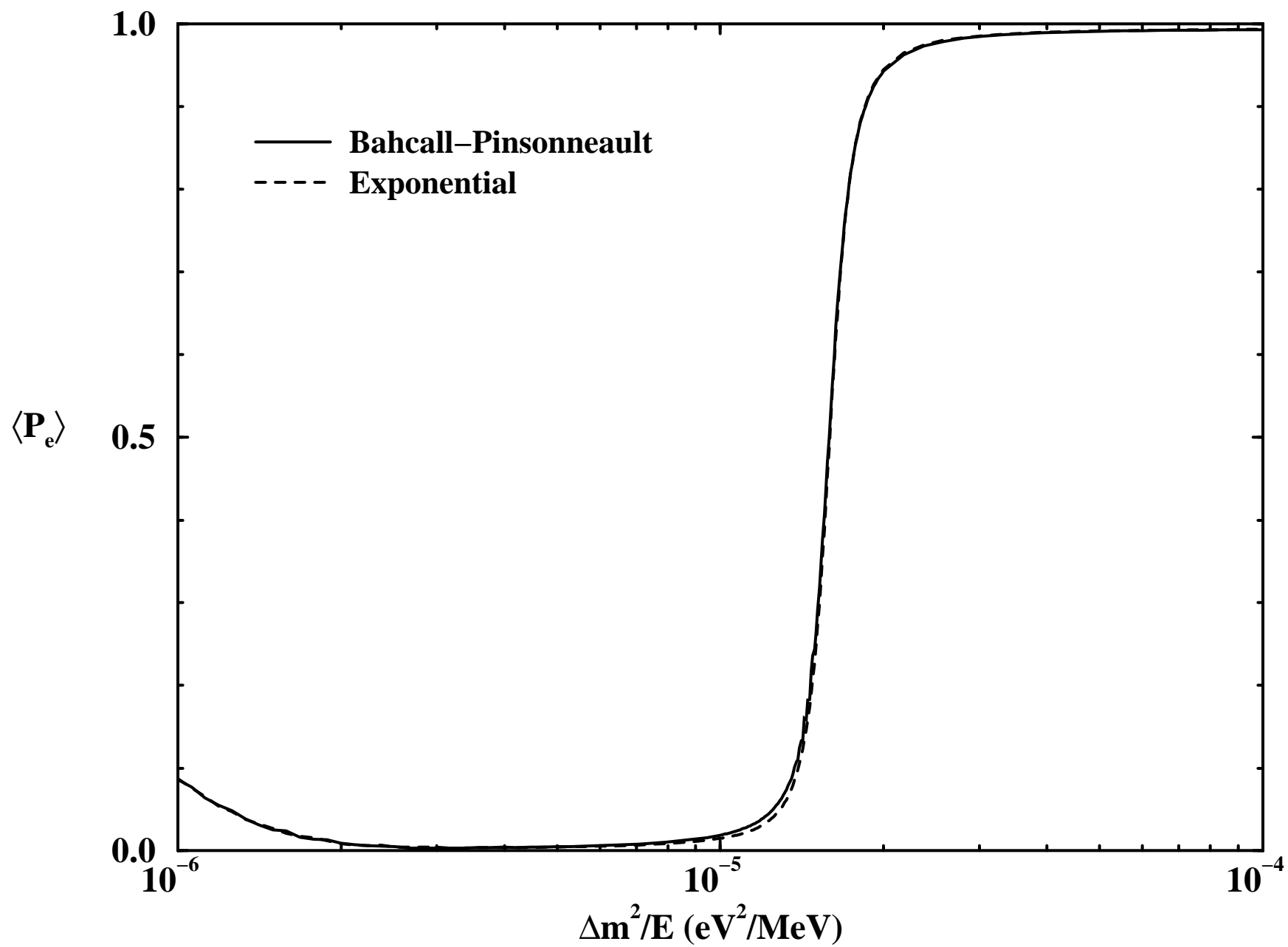


Figure 4c

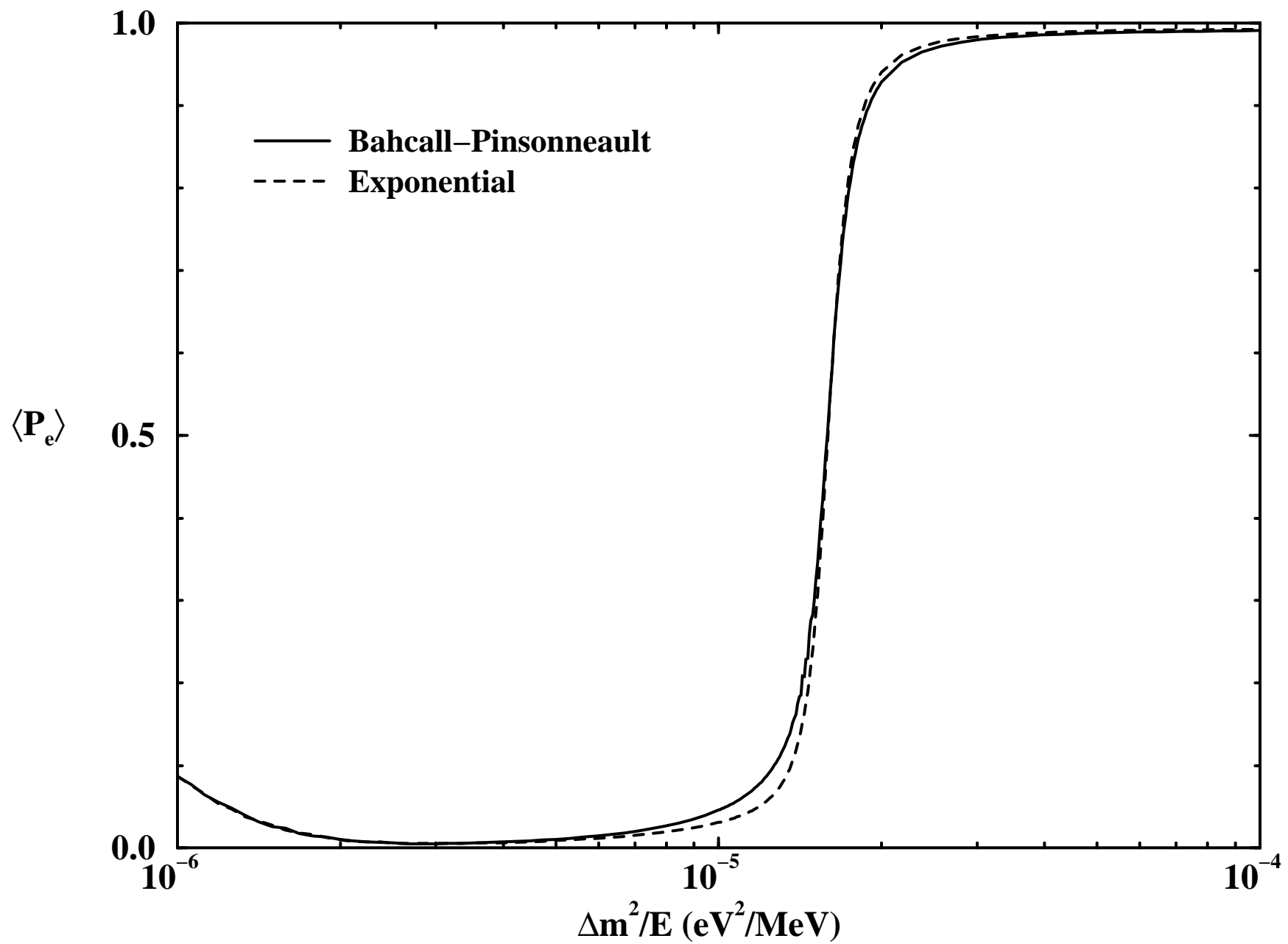


Figure 4d

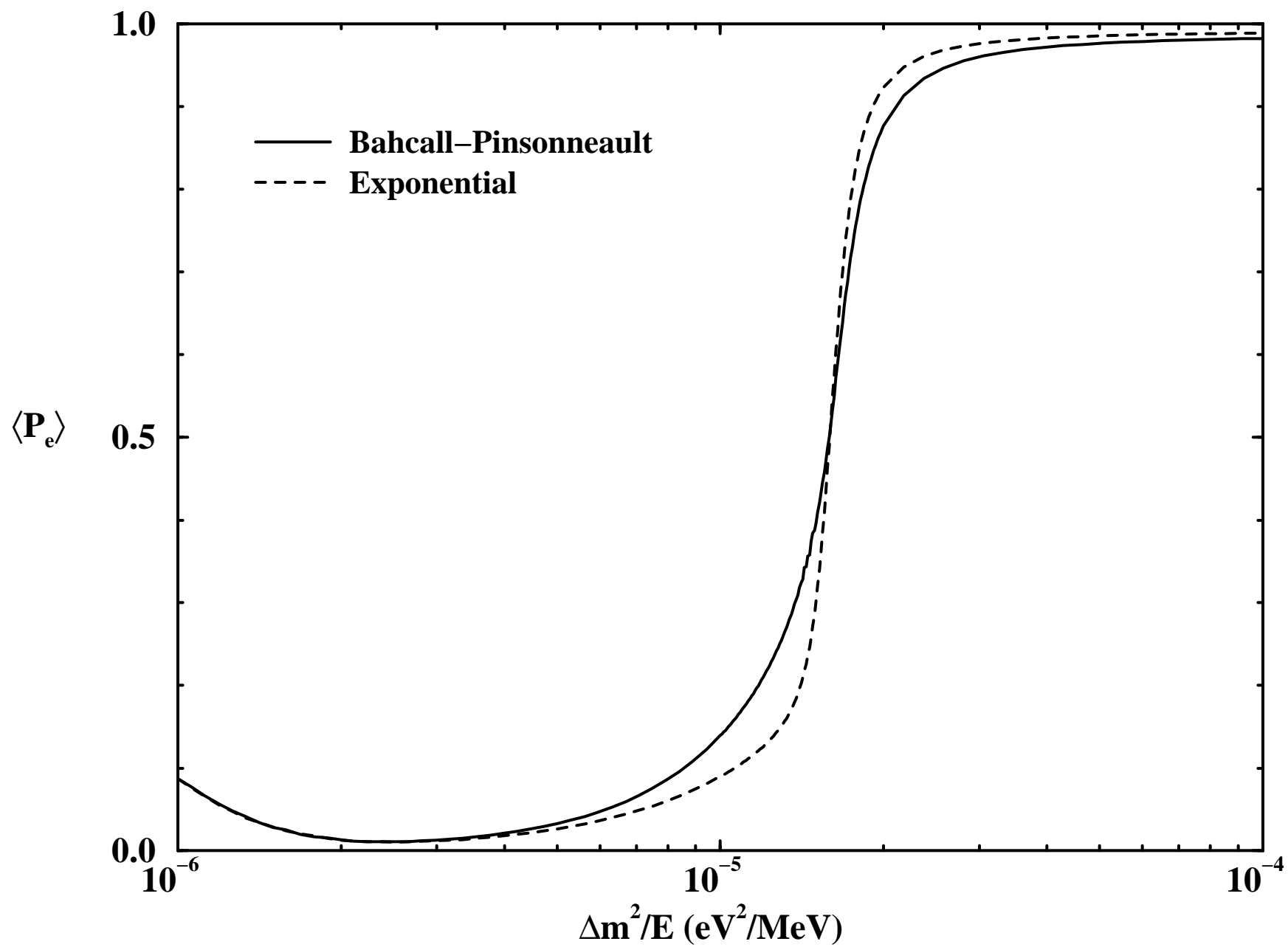


Figure 4e

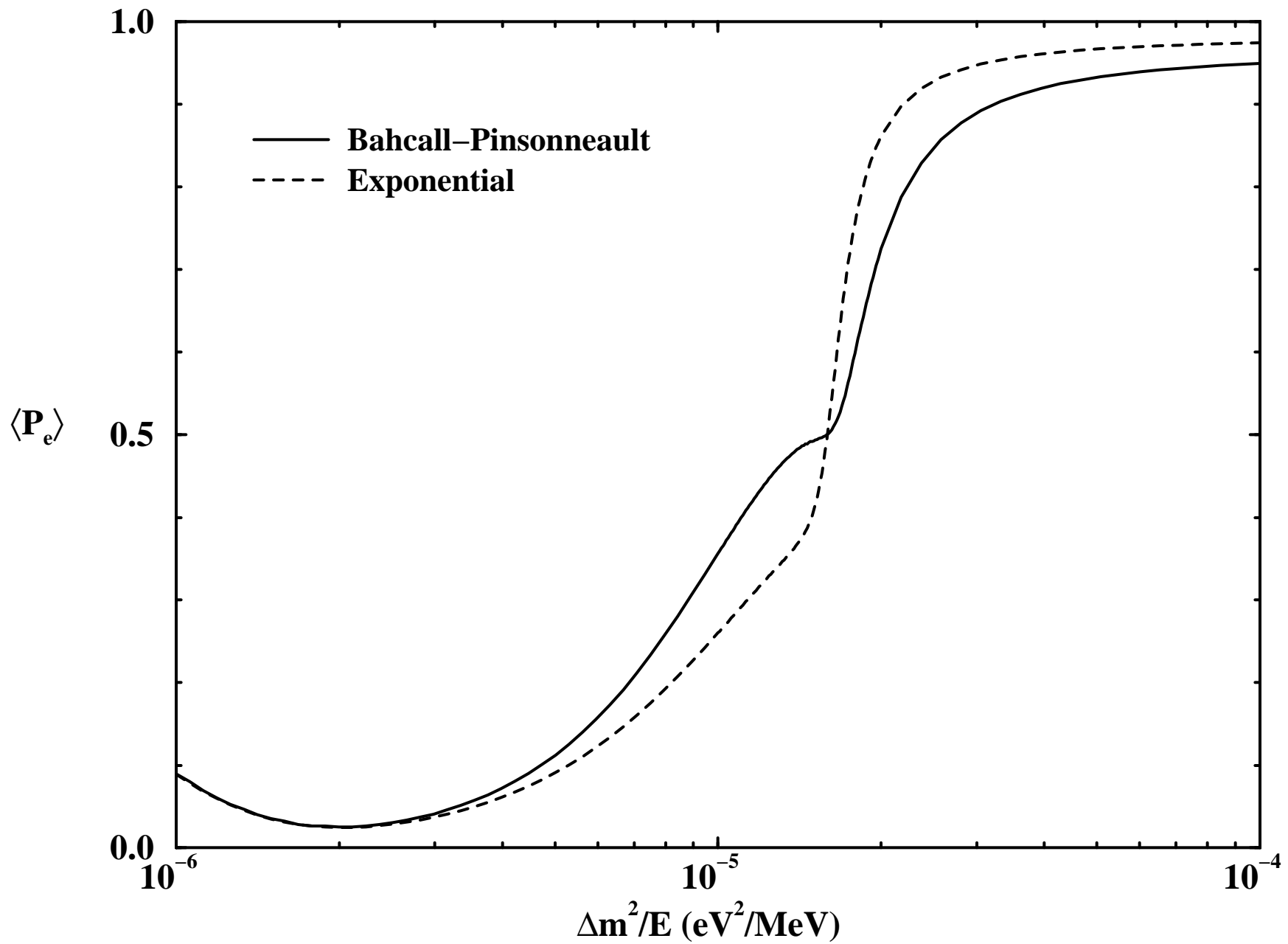


Figure 5a

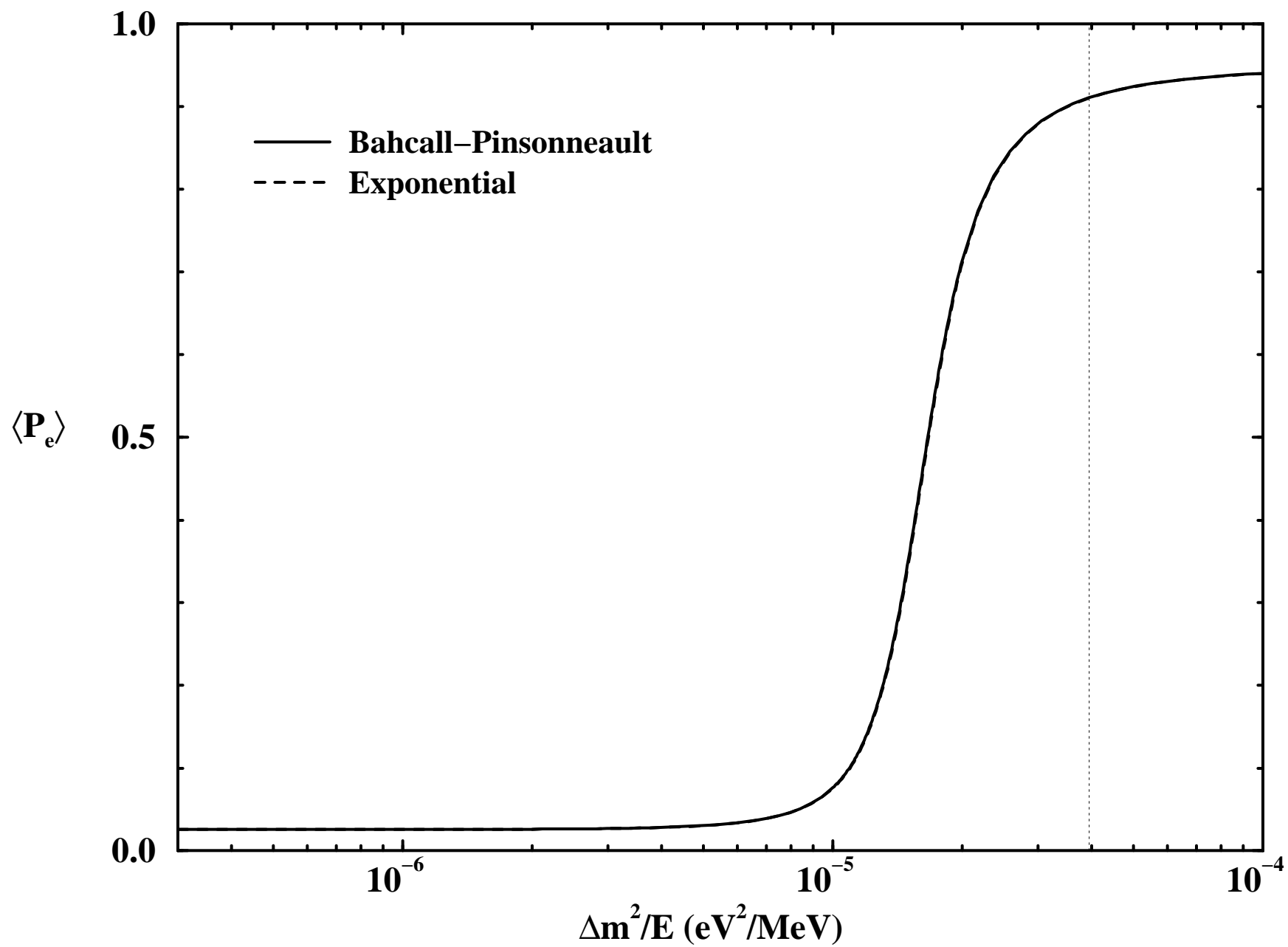


Figure 5b

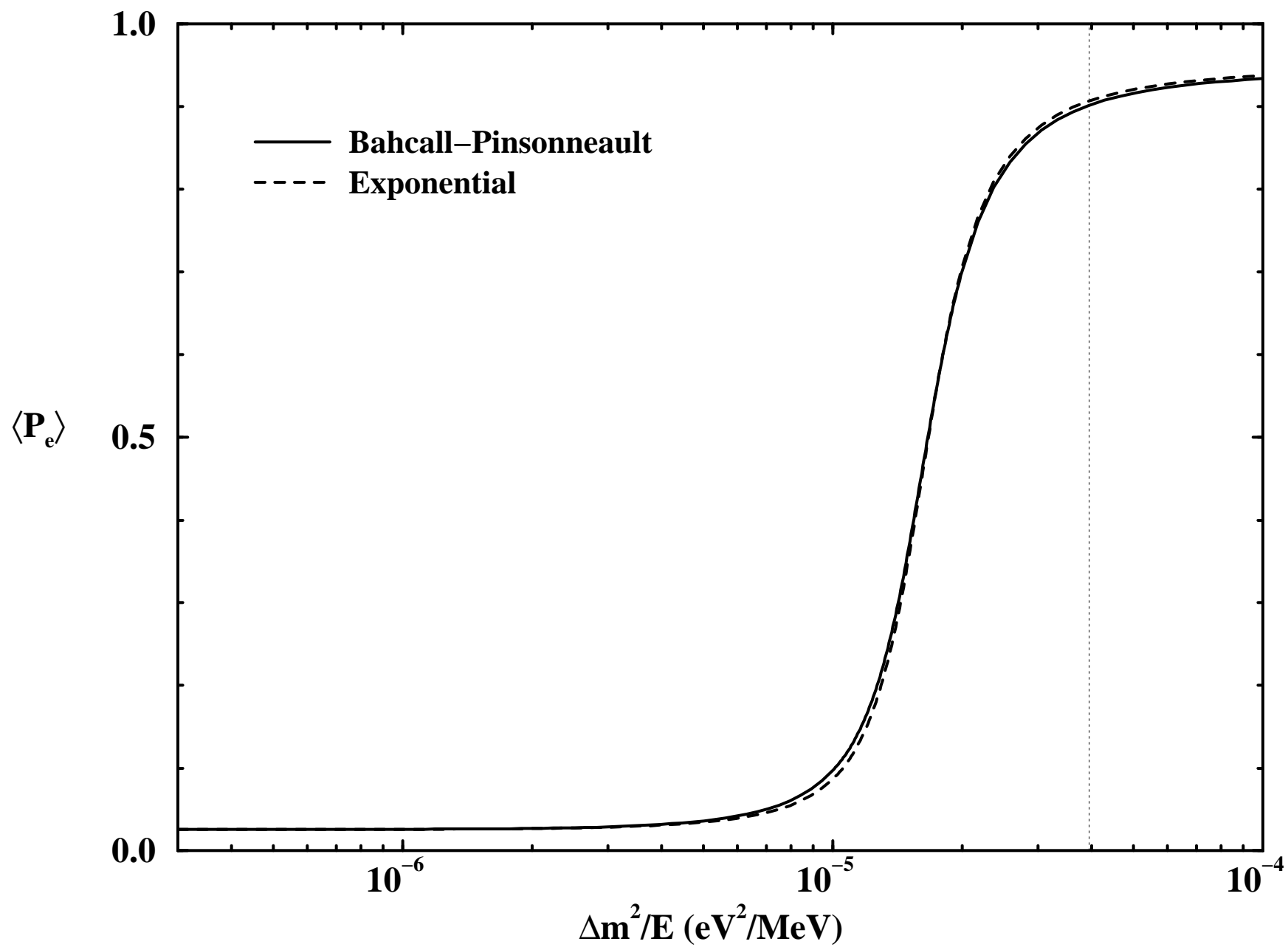


Figure 5c

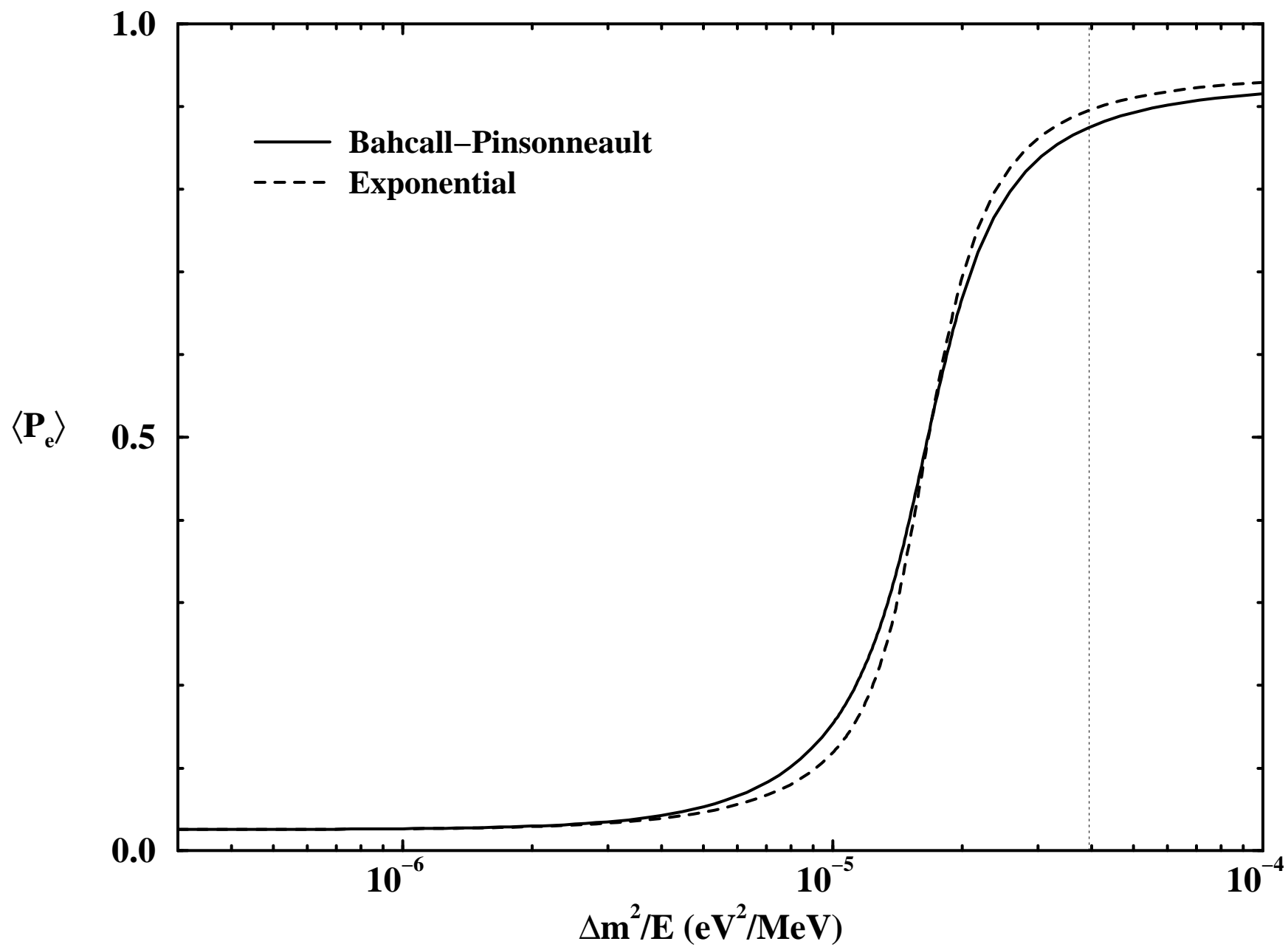


Figure 5d

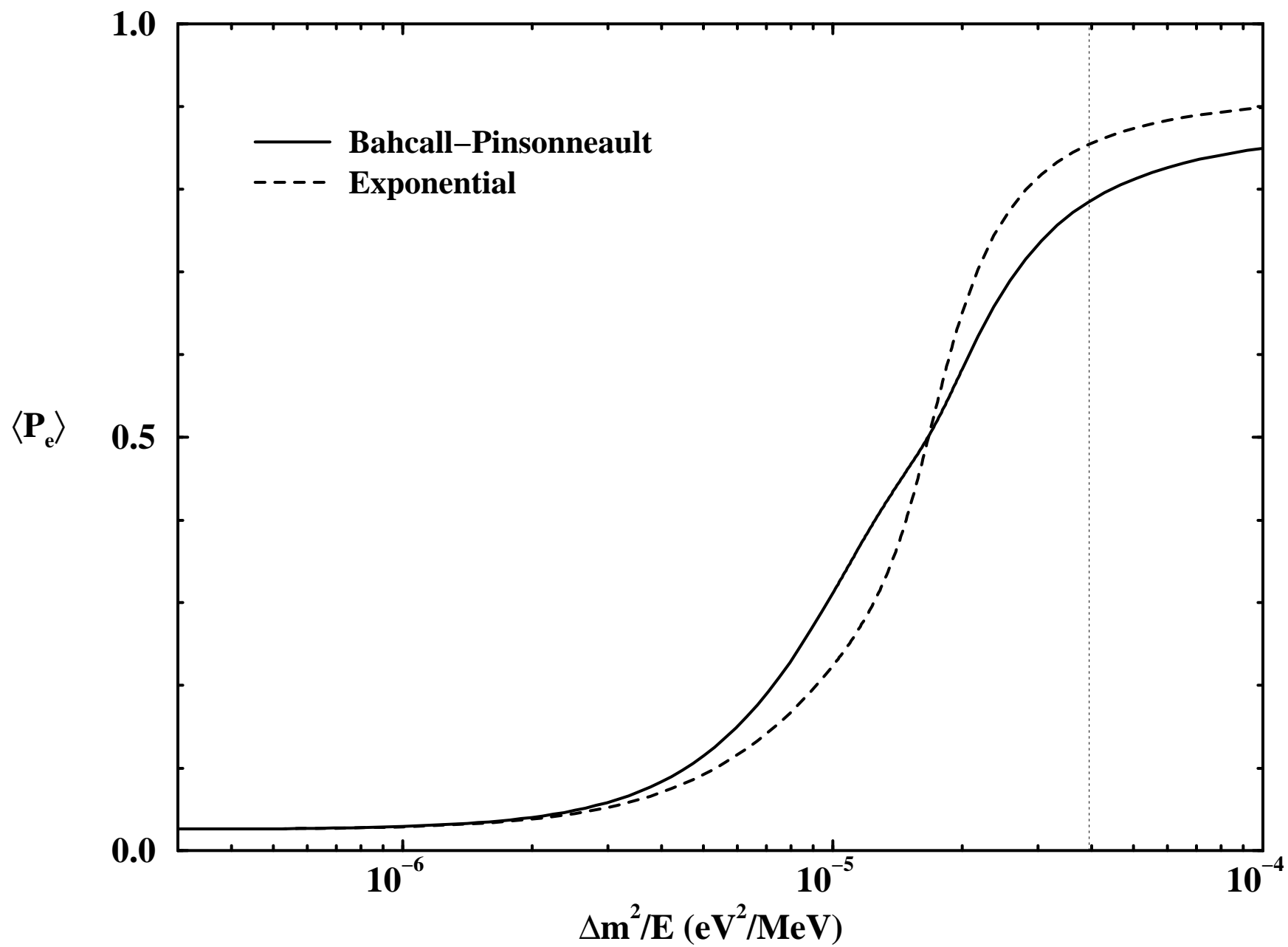


Figure 5e

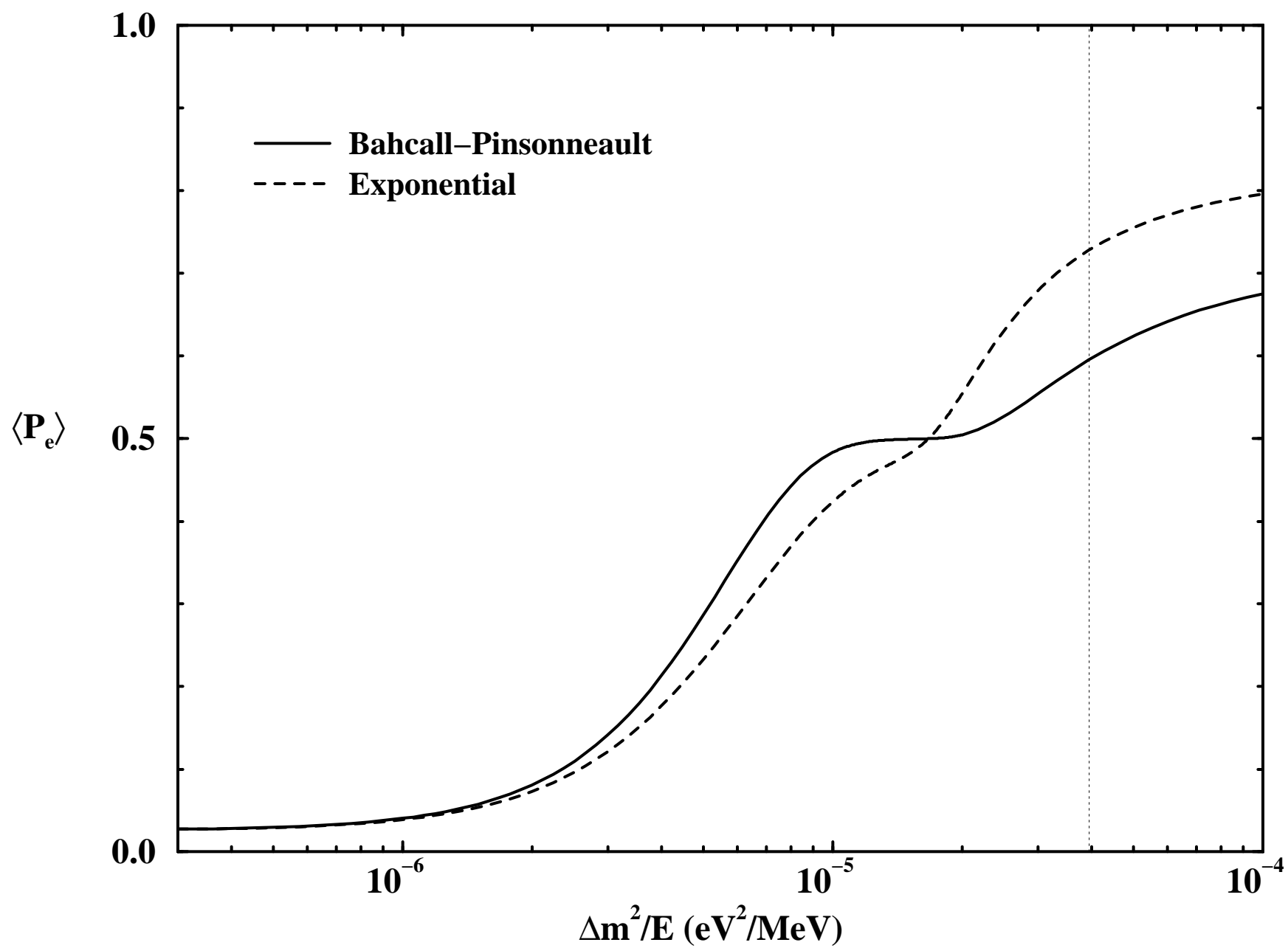


Figure 6a

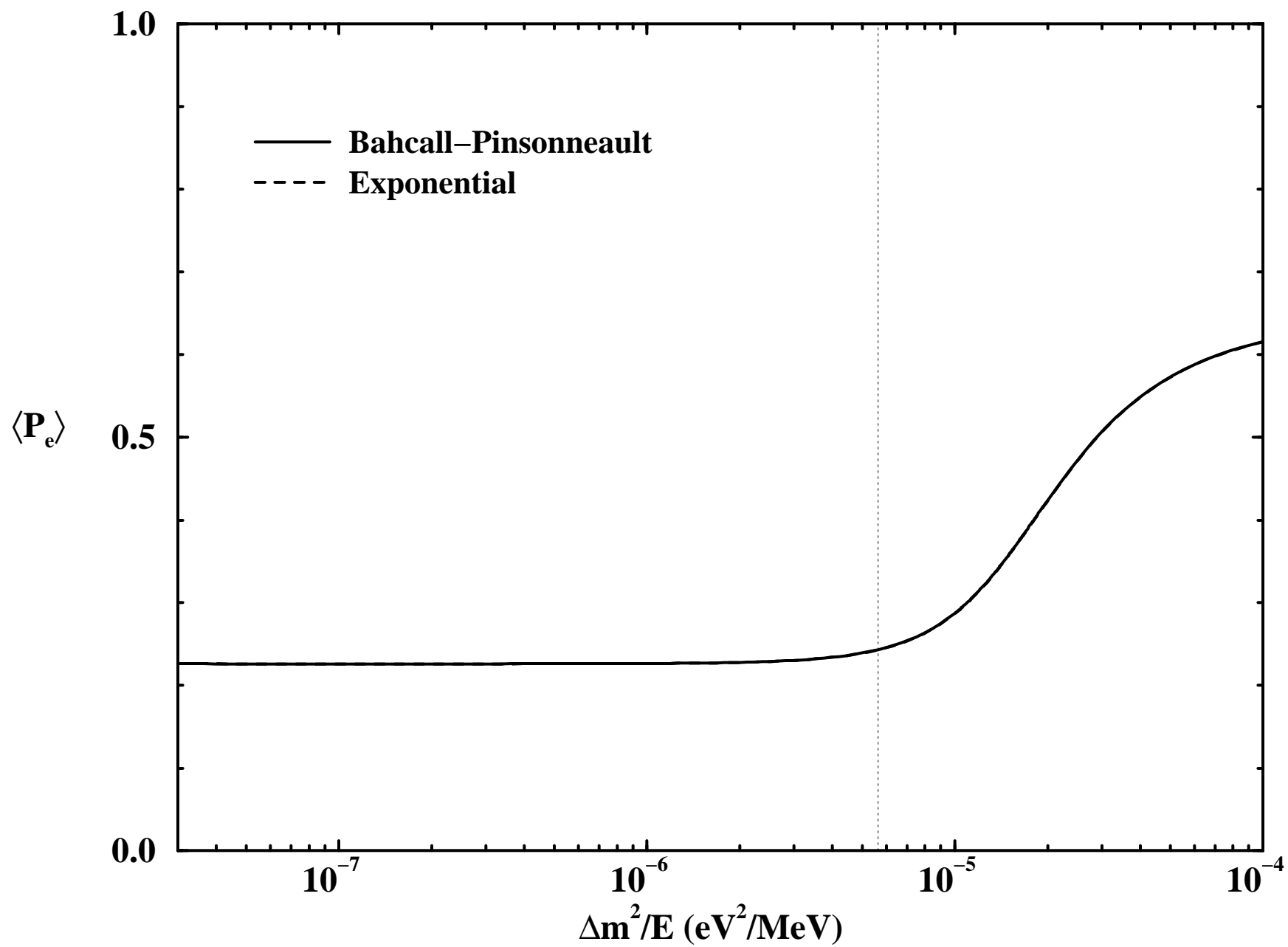


Figure 6b

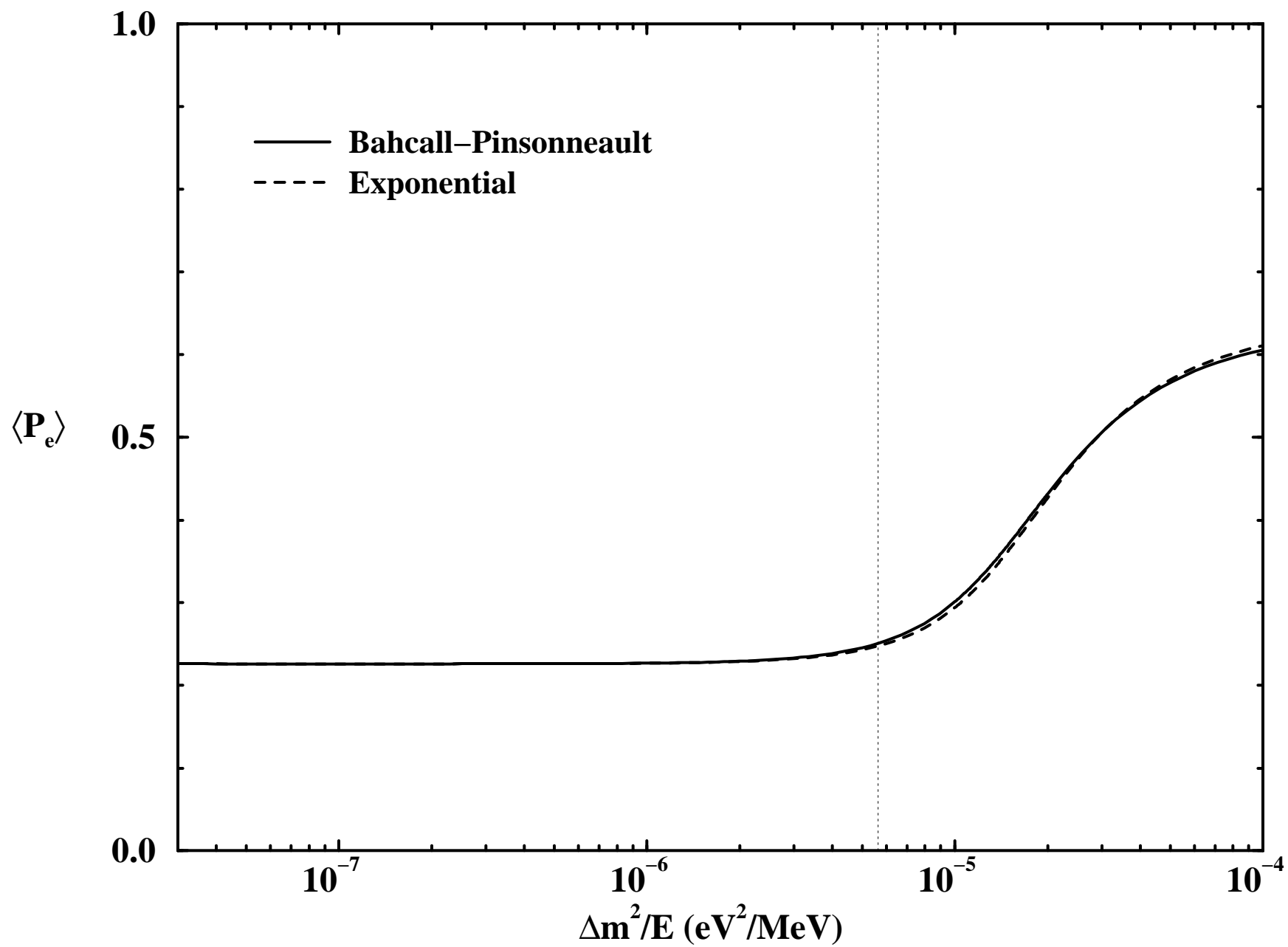


Figure 6c

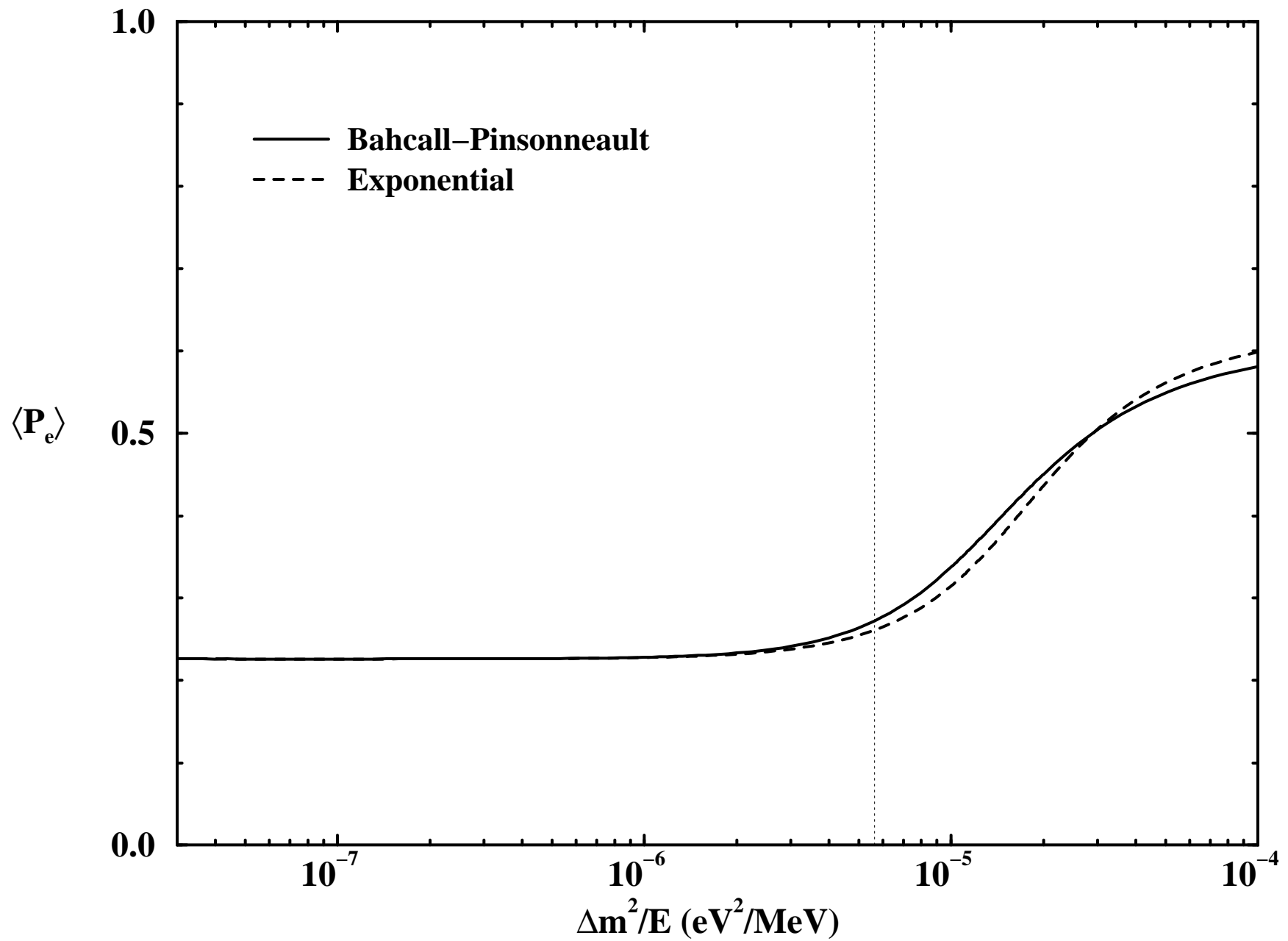


Figure 6d

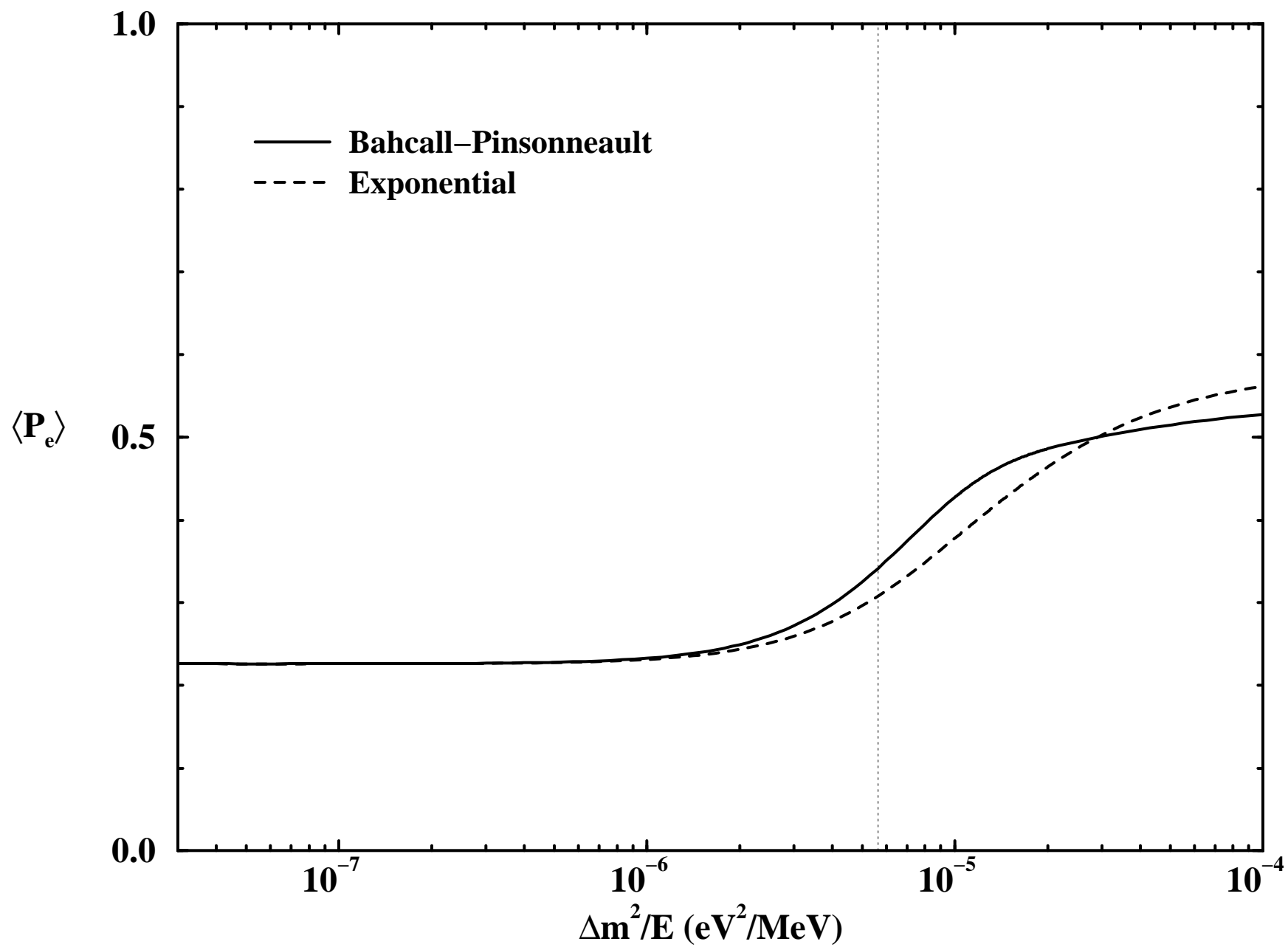


Figure 6e

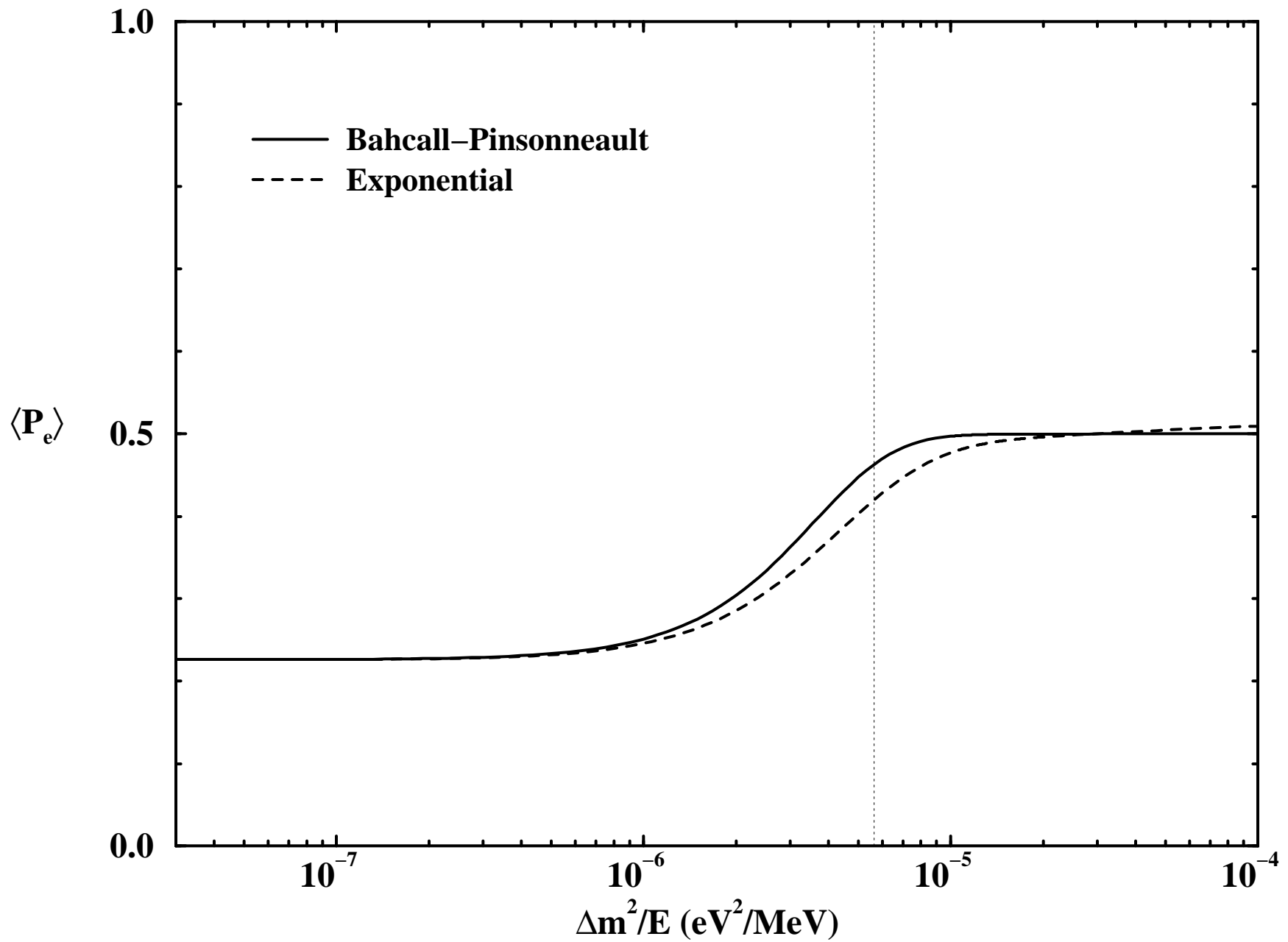


Figure 7

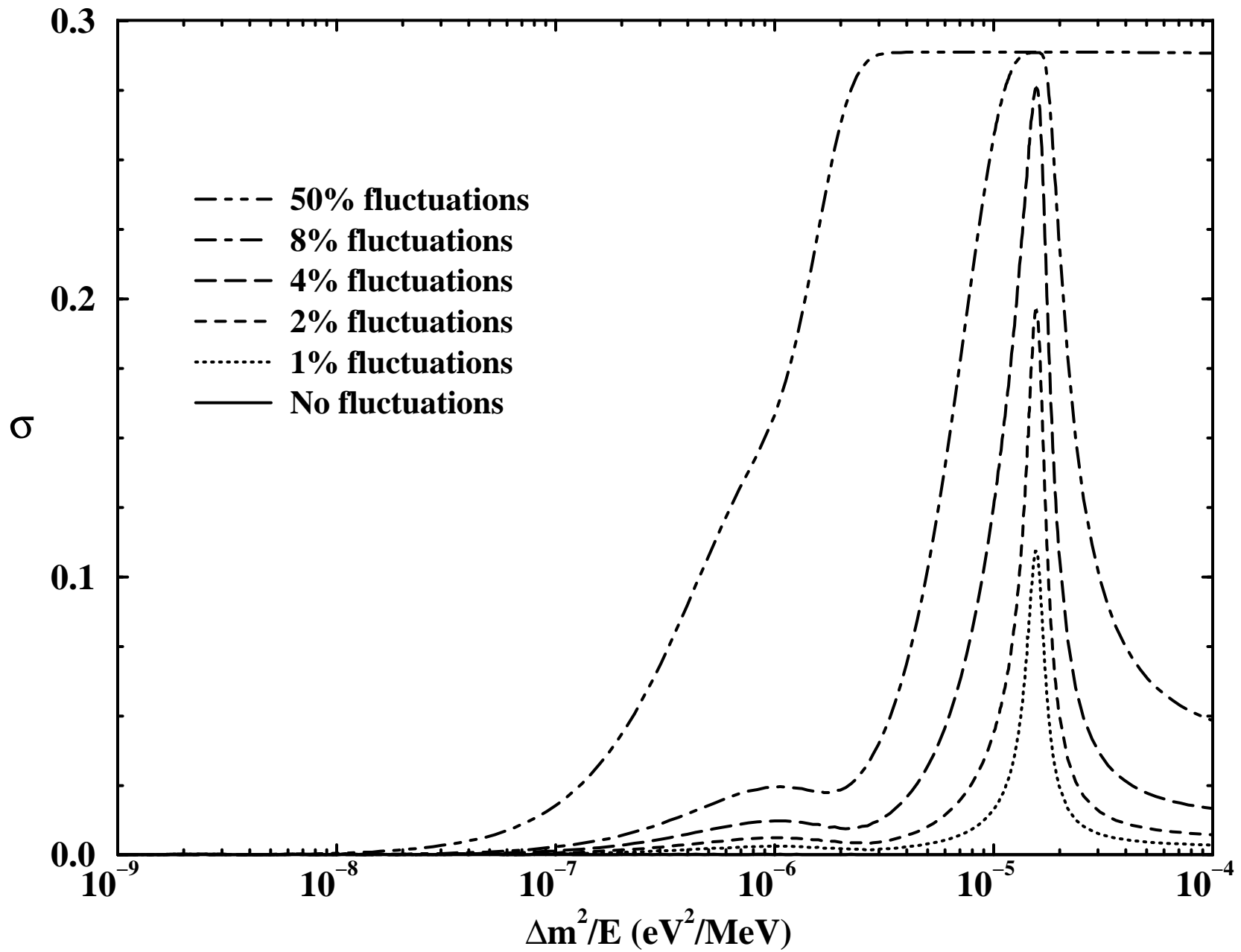


Figure 8

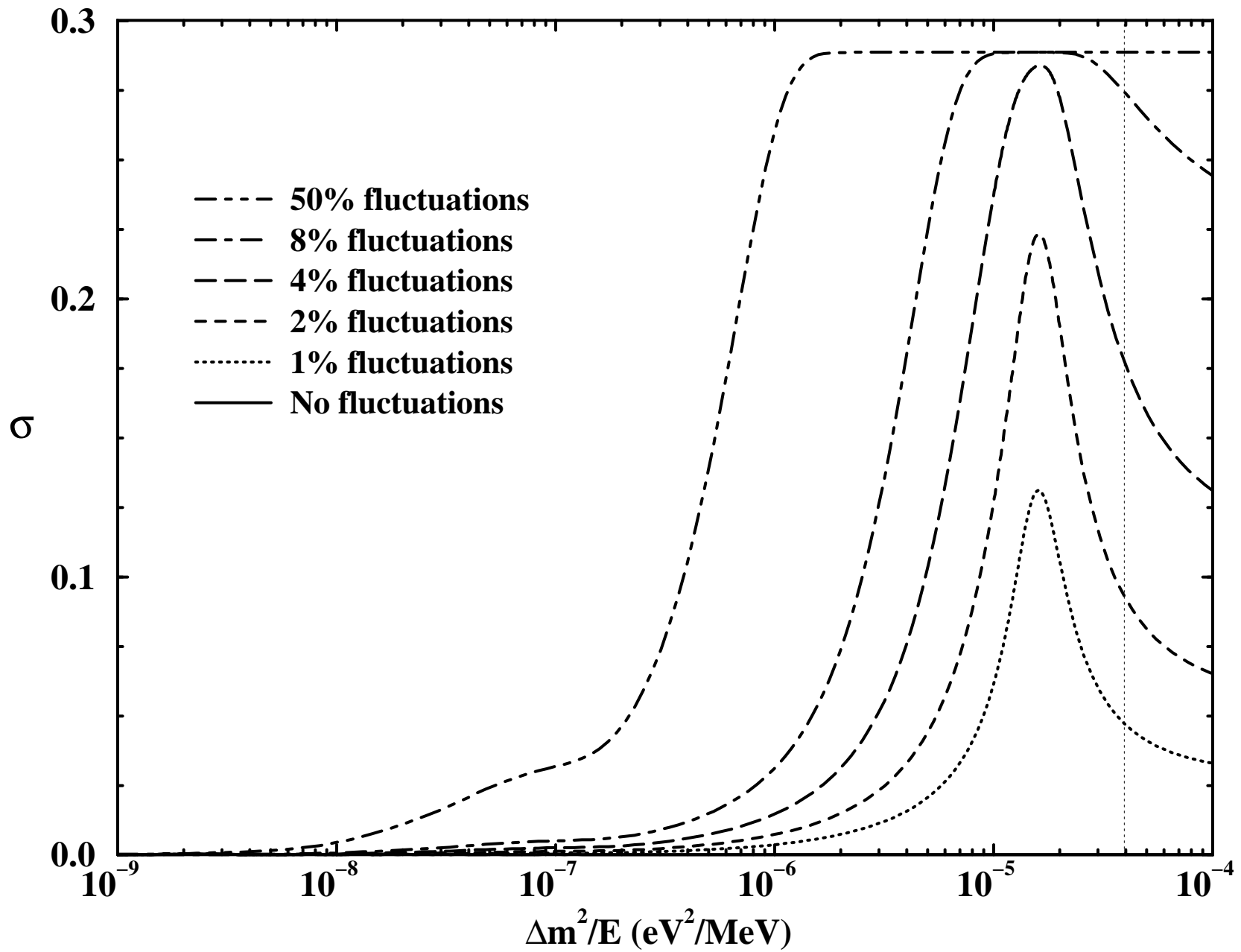


Figure 9

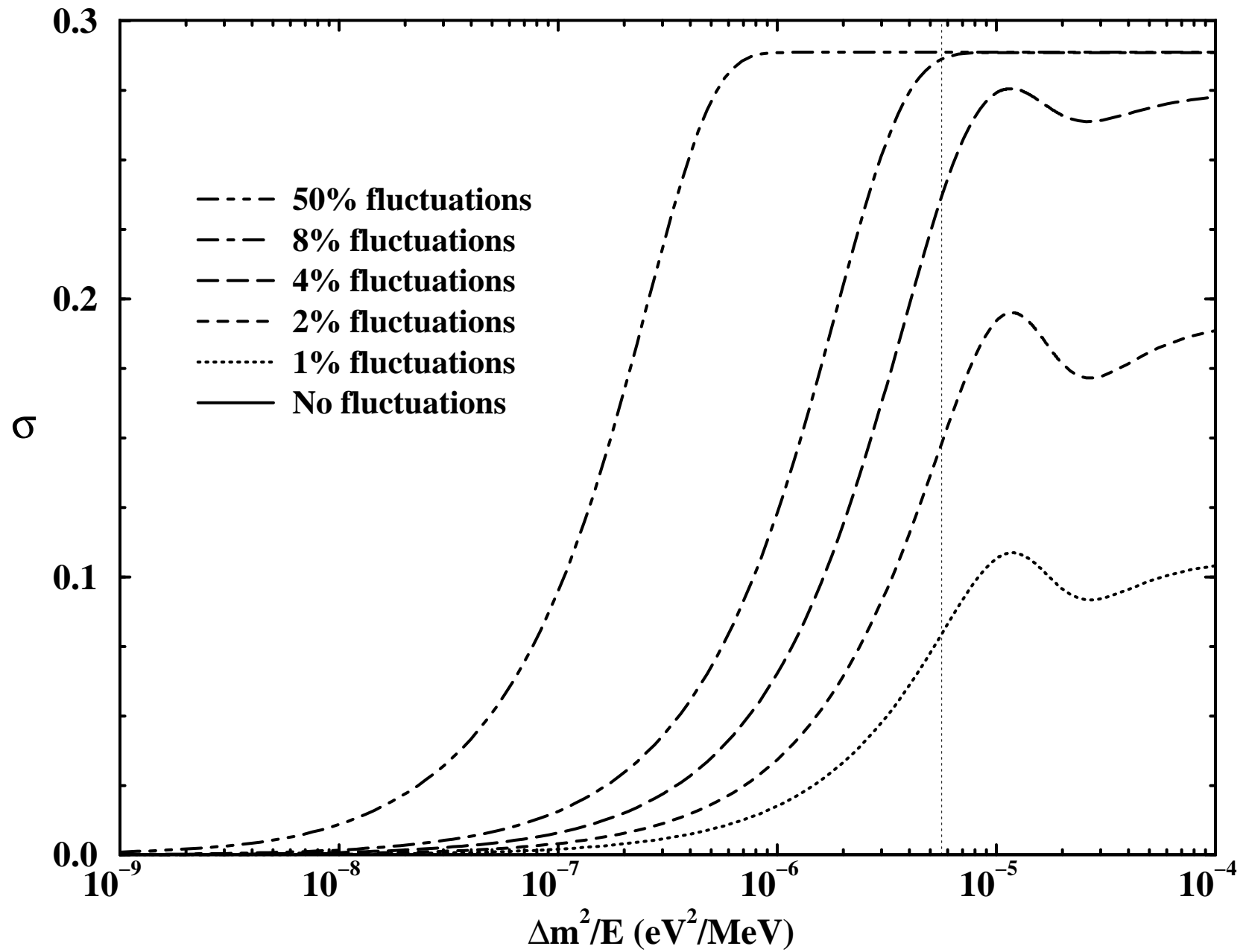


Figure 10

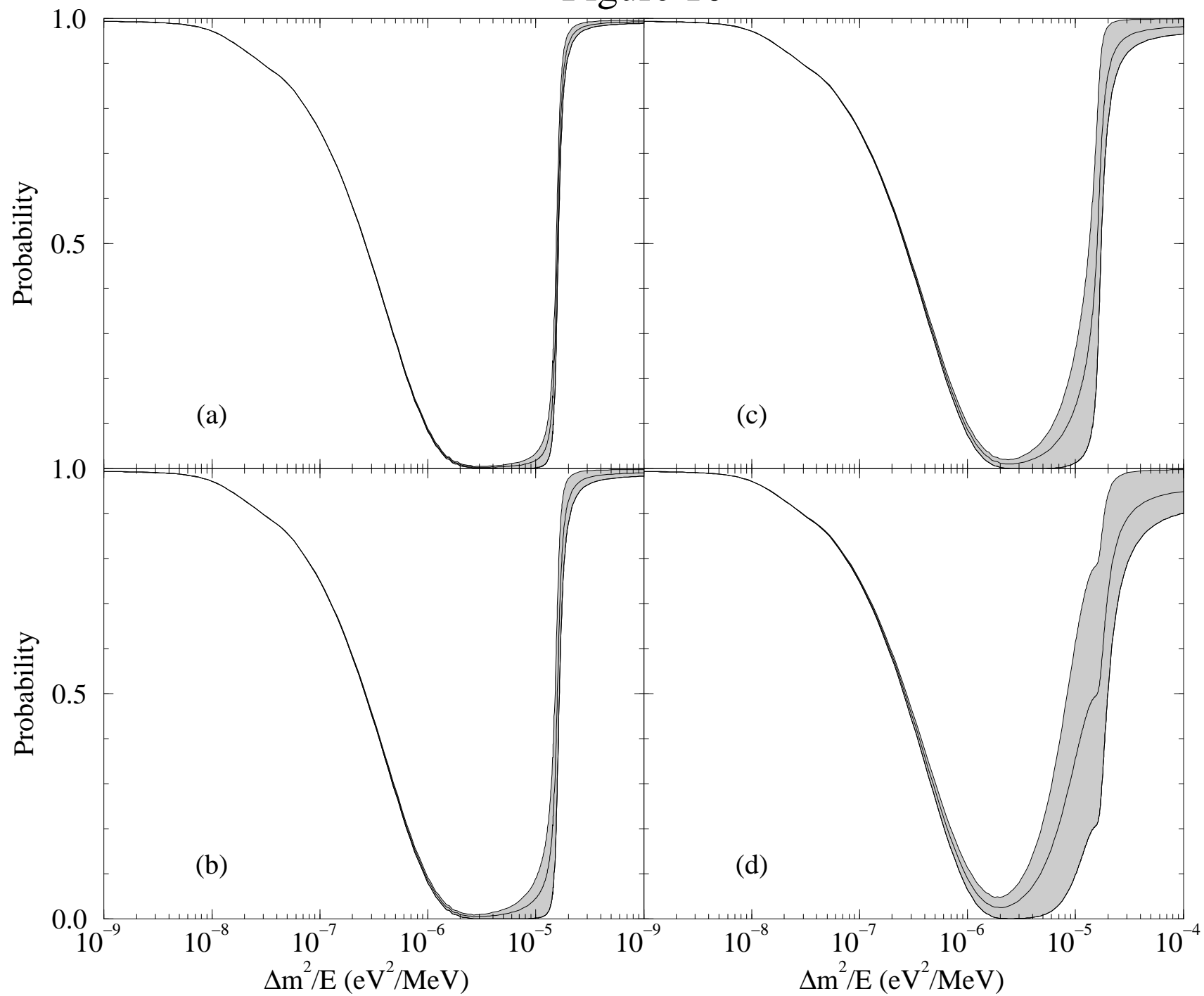


Figure 11

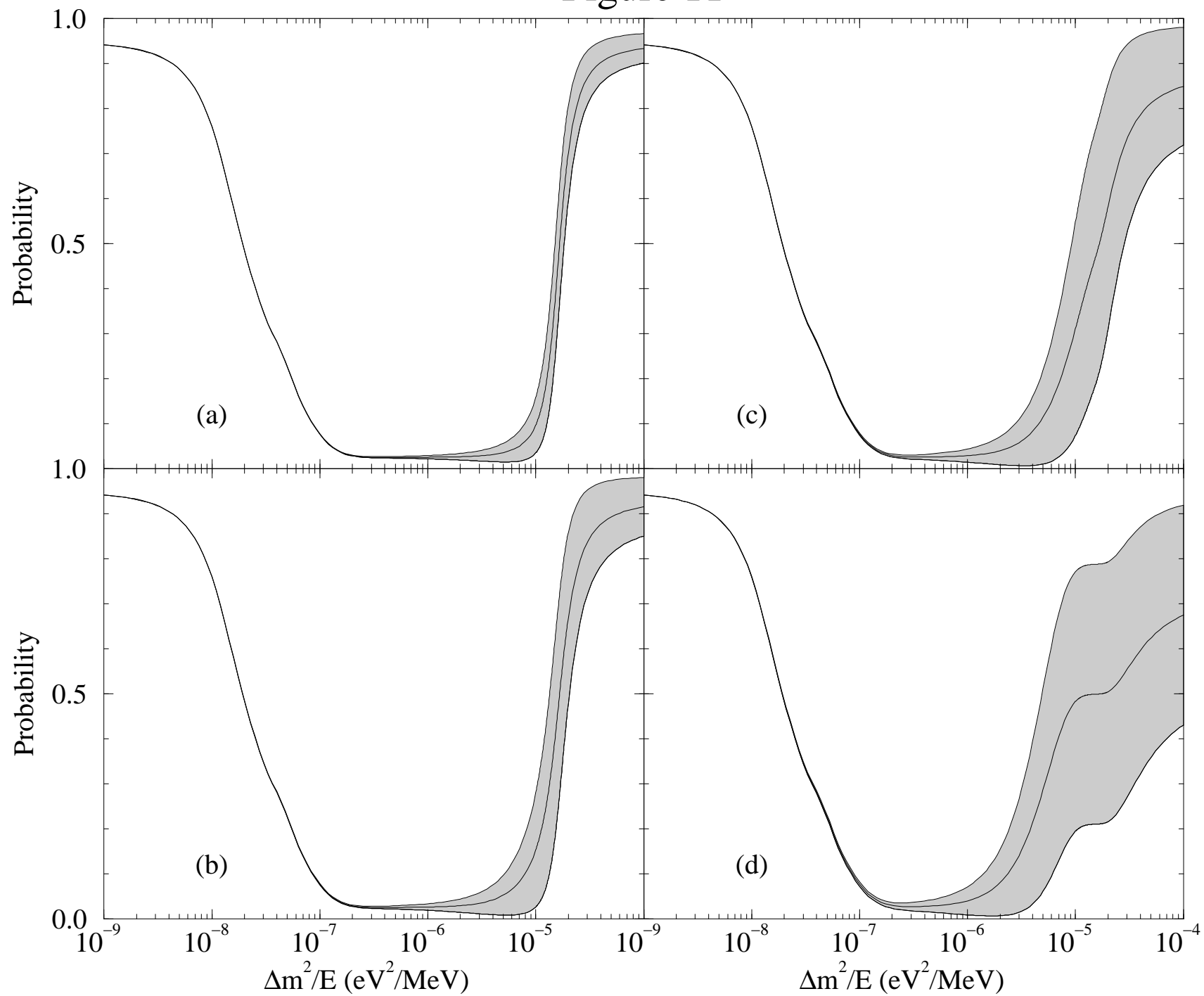


Figure 12

